LBL-36676
UC-401
Preprint

Lawrence Berkeley Laboratory
UNIVERSITY OF CALIFORNIA

CHEMICAL SCIENCES DIVISION

Submitted to Inorganic Chemistry

Multinuclear NMR, Raman, EXAFS, and X-ray Diffraction Studies of Uranyl Carbonate Complexes in Near-neutral Aqueous Solution. X-ray Structure of $[C(NH_2)_3]_6[(UO_2)_3(CO_3)_6]\cdot 6.5H_2O$

P.G. Allen, J.J. Bucher, D.L. Clark, N.M. Edelstein, S.A. Ekberg, J.W. Gohdes, E.A. Hudson, N. Kaltsoyannis, W.W. Lukens, M.P. Neu, P.D. Palmer, T. Reich, D.K. Shuh, C.D. Tait, and B.D. Zwick

December 1994

Prepared for the U.S. Department of Energy under Contract Number DE-AC03-76SF00098

DISCLAIMER

LBL-36676
LA-UR-93-3950
UC-401

Multinuclear NMR, Raman, EXAFS, and X-ray Diffraction Studies of Uranyl Carbonate Complexes in Near-neutral Aqueous Solution. X-ray Structure of $[C(HN_2)_3]_6[(UO_2)_3(CO_3)_6]\cdot 6.5H_2O$

P.G. Allen,[1a,c] J.J. Bucher,[1a] D.L. Clark,*[1b,c] N.M. Edelstein,*[1a,c] S.A. Ekberg,[1b] J.W. Gohdes,[1b] E.A. Hudson,[1c] N. Kaltsoyannis,[1a] W.W. Lukens,[1a] M.P. Neu,[1b] P.D. Palmer[1b], T. Reich,[1d] D.K. Shuh,[1a] C.D. Tait,[1b] and B.D. Zwick[1b]

[1a]Chemical Sciences Division, Lawrence Berkeley Laboratory, University of California, Berkeley, CA 94720
[1b]Chemical Science and Technology Division, and Nuclear Materials Technology Division, Los Alamos National Laboratory, Los Alamos, NM 87545
[1c]G.T. Seaborg Institute for Transactinium Science, Lawrence Livermore National Laboratory, Livermore, CA 94551
[1d]Forschungszentrum Rossendorf e. V., Institut für Radiochemie, Postfach 51 01 19, D-01314 Dresden, Germany

December 1994

This work was supported by the Office of Basic Energy Sciences, Division of Chemical Sciences, U.S. Department of Energy under Contract No. W-7405-ENG-36 with the University of California, and by the Yucca Mountain Site Characterization Project Office as part of the Civilian Radioactive Waste Management Program managed by the U.S. Department of Energy, Nevada Operations Office, through the U.S. Department of Energy Contract No. DE-AC03-76SF00098.

Abstract

^{13}C and ^{17}O NMR, and Raman spectroscopies were used to monitor the fractions of $UO_2(CO_3)_3^{4-}$ (**1**) and $(UO_2)_3(CO_3)_6^{6-}$ (**2**) in aqueous carbonate solutions as a function of pH, ionic strength, carbonate concentration, uranium concentration, and temperature. The multinuclear NMR and Raman data are consistent with the formation of $(UO_2)_3(CO_3)_6^{6-}$. The pH dependence of the ^{13}C NMR spectra was used to determine the equilibrium constant for the reaction $3UO_2(CO_3)_3^{4-} + 3H^+ \rightleftharpoons (UO_2)_3(CO_3)_6^{6-} + 3HCO_3^-$, log K = 18.1(±0.5) at I_m = 2.5 m and 25°C, and corresponds to $\log\beta_{36}$ = 55.6(±0.5) for the reaction $3\ UO_2^{2+} + 6\ CO_3^{2-} \rightleftharpoons (UO_2)_3(CO_3)_6^{6-}$ under the same conditions. Raman and IR spectra showed ν_1 = 831.6 cm^{-1} (Raman active) and ν_3 = 911 cm^{-1} (IR active) U=O stretching bands for **1**, and ν_1 = 812.5 cm^{-1} and ν_3 = 889 cm^{-1} for trimeric $(UO_2)_3(CO_3)_6^{6-}$, **2**. EXAFS data from solid $[C(NH_2)_3]_6[(UO_2)_3(CO_3)_6]$ and a solution of $(UO_2)_3(CO_3)_6^{6-}$ suggest that the same uranium species is present in both the solid and solution states. Fourier transforms of the EXAFS spectra of both solid and solution samples revealed 5 well-resolved peaks corresponding to nearly identical near-neighbor distances for solid and solution samples of **2**. Fitting of these peaks yields U-O (uranyl) = 1.79, U-O (carbonate) = 2.45, U--C = 2.90, U--O (terminal carbonate) = 4.16, and U--U = 4.91 Å for the solid, and similar distances for the solution sample. The peak at 4.75 Å in both Fourier transforms (uncorrected for phase shift) corresponds to the U--U interaction at 4.91 Å, a conclusion which is supported by the absence of this peak in the Fourier transform of the crystalline monomeric $K_4[UO_2(CO_3)_3]$. Multiple scattering along the uranyl vector is believed to play a significant role in the EXAFS of all three systems. The EXAFS data are consistent with the trimeric uranyl carbonate species indicated by NMR spectroscopy. Single crystals of $[C(NH_2)_3]_6[(UO_2)_3(CO_3)_6]\cdot 6.5H_2O$ were obtained from a solution that contained stoichiometric amounts of uranyl nitrate, guanidinium carbonate, and an excess of guanidinium nitrate at pH 6.5 under a CO_2 atmosphere. The solid state molecular structure of $[C(NH_2)_3]_6[(UO_2)_3(CO_3)_6]\cdot 6.5H_2O$ contains a planar D_{3h} trimetallic $(UO_2)_3(CO_3)_6^{6-}$ anion, the

structure that Åberg and coworkers originally proposed for the trimeric solution species. The trimetallic anion contains three uranium atoms and all six carbonate ligands in the molecular plane with three uranyl oxygen atoms above, and three below the plane. Uranyl U=O distances average 1.78(1) Å, while U-O distances to the carbonate oxygen atoms average 2.41(1) Å for terminal, and 2.48(1) Å for bridging ligands. Particularly significant is the average nonbonding U--U distance of 4.97 Å which compares favorably to the 4.91 Å distance seen in the EXAFS analysis. The molecule crystallizes in the triclinic space group P1bar, with a = 6.941(2), b = 14.488(2), c = 22.374(2) Å, α = 95.63(2), β = 98.47(2), γ = 101.88(2)°, R = 0.0547, R_w = 0.0616, V = 2157.4 $Å^3$, d_{calc} = 2.551 g cm^{-3}, Z = 2.

Introduction

Carbonate and bicarbonate are common anions found in significant concentrations in many natural waters, and are exceptionally strong complexation agents for actinide ions.[2-5] Therefore, carbonate complexation may play an important role in migration of actinide ions from a nuclear waste repository or in accidental site contamination.[6,7] The stability of actinide carbonate complexes is reflected in the formation of naturally-occurring uranyl carbonate minerals such as rutherfordine, $UO_2(CO_3)$,[8] leibigite, $Ca_2[UO_2(CO_3)_3]\cdot 10\text{-}11H_2O$,[9] and andersonite, $Na_2Ca[UO_2(CO_3)_3]\cdot 6H_2O$.[10]

Actinide carbonate systems can be quite complicated because several different complex ions can exist in rapid equilibria with one another and with the uncomplexed ion or hydrolyzed species. The uranyl carbonate system is by far the most extensively studied of all actinide carbonate systems.[11-28] The composition and molecular structure of the tris-carbonato complex of formula $AnO_2(CO_3)_3^{4-}$ is well-established for the light actinides U, Np, Pu, and Am.[10,17,21,29-36] For bis-carbonato complexes of empirical formula $AnO_2(CO_3)_2^{2-}$, a trimeric species of composition $[AnO_2(CO_3)_2]_3^{6-}$ has been reported for An = U, Np, and Pu.[17,19,37] For uranyl, this trimer is strongly stabilized in solutions of high ionic strength, and is thought to be responsible for the very high solubility of $AnO_2CO_{3(s)}$ in carbonate solutions, and thus may be important in aquatic transport of actinyl ions via carbonate complexation. The molecular structure of the monomeric $UO_2(CO_3)_3^{4-}$, based on single crystal X-ray diffraction is shown schematically in **1**.[10]

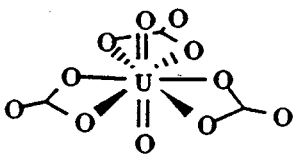

1

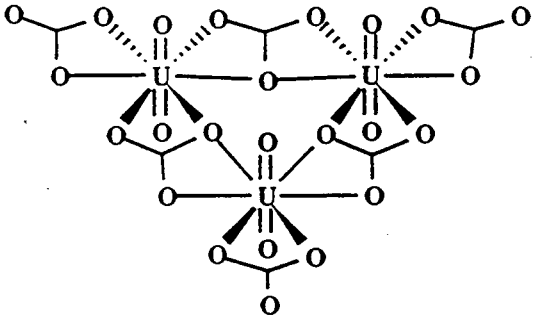

2

Ciavatta *et al.* were the first to propose the presence of $(UO_2)_3(CO_3)_6^{6-}$ to model potentiometric (emf) titration data.[17] These workers also reported two ^{13}C NMR resonances consistent with the structure proposed in **2**.[25] Several years later, Åberg *et al.* used X-ray scattering data from a solution concentrated in the $(UO_2)_3(CO_3)_6^{6-}$ cluster to propose the structural unit shown in **2**.[25] Subsequently, Ferri *et al.* reported five ^{17}O NMR signals between δ 1130 - 1095 ppm in the expected 2:2:2:1:1 ratio,[38] confirming the solution structure of $(UO_2)_3(CO_3)_6^{6-}$ as that shown in **2**. However, we note that all five ^{17}O resonances reported for $(UO_2)_3(CO_3)_6^{6-}$ appear in the uranyl (O=U=O) chemical shift region of the ^{17}O NMR spectrum. Since carbonate oxygen signals should appear near 200 ppm in the spectrum,[39] the signals reported by Ferri *et al.* cannot be due to the five types of oxygen present in the proposed trimer structure. Either there were multiple uranyl-containing species present in solution, or the structure of the trimer is more complex than originally proposed. These observations prompted the present multinuclear NMR, Raman, EXAFS and single crystal x-ray diffraction study of the uranyl carbonate system.

Results and Discussion.

In this paper, pH refers to the negative log of an approximate activity of the H^+ ion based on the reading of a pH meter calibrated using commercial buffers. We use p[H] to mean the negative log of the H^+ concentration using a pH meter calibrated with solutions of appropriate ionic strength and known hydrogen ion concentration, as described in the experimental section.

Spectroscopic Characterization.

^{13}C NMR. The uranyl carbonate system was studied using ^{13}C NMR spectroscopy of ^{13}C-enriched $UO_2(CO_3)_3^{4-}$ at 0.2 and 0.05 *M* concentrations and ionic strengths of 4.0 and 2.5m. Initial solutions were prepared with a carbonate-to-metal ratio of 3:1 in order to favor the formation of the monomeric $UO_2(CO_3)_3^{4-}$ complex (**1**).[7] Careful titration with $HClO_4$ leads to protonation

of the carbonate ligand resulting in a decrease in the carbonate:uranyl ratio to 2:1 as proposed by Ciavatta *et al.*, and outlined in eq 1.[17, 25]

$$3\ UO_2(CO_3)_3^{4-} + 6H^+ \rightleftharpoons (UO_2)_3(CO_3)_6^{6-} + 3\ CO_2 + 3\ H_2O \qquad (1)$$

Aliquots were removed at various stages of the titration, flame-sealed in glass NMR tubes, and allowed to equilibrate for approximately 48-72 hours. The ^{13}C NMR spectra were recorded at 23 °C and a representative series is shown in Figure 1a. At pH ≥ 8.0, a single ^{13}C NMR resonance is observed (0.2*M* solution) at δ 165.2 ppm (Figure 1a) and is assigned to the single type of carbonate ligand in monomeric $UO_2(CO_3)_3^{4-}$ as observed previously by others.[25-28] At pH 7.5 a new ^{13}C resonance appears at δ 166.2 ppm, and the original resonance at δ 165.2 ppm begins to show some line-broadening. At pH 7.0, a well-defined shoulder at δ 164.9 ppm can be seen on the side of the original NMR resonance line centered at δ 165.2 ppm. With decreasing pH, the original monomer resonance at δ 165.2 disappears and the two new resonances (δ 164.9 and δ 166.2) of the second species grow in as shown in Figure 1a. The spectrum at pH 6.0 is nearly identical with the spectrum reported by Åberg et al.[25] Notably, one of the NMR signals observed at pH 6.0 is relatively sharp, while the other is broad, suggesting that chemical exchange is occurring on the timescale of the NMR experiment. When the ^{13}C NMR spectra of the uranyl carbonate system was recorded at 0 °C, chemical exchange was slowed and the line-width of the terminal carbonate resonances in both monomer and the new (presumably trimeric) species sharpened. A stacked plot of this same sample recorded at 0 °C is shown in Figure 1b.

The monomeric $UO_2(CO_3)_3^{4-}$ (**1**) has only one type of carbonate ligand environment, and gives rise to a single ^{13}C NMR resonance (δ 165.2 ppm) as seen in Figure 1 at pH 8.0. The proposed structure for $(UO_2)_3(CO_3)_6^{6-}$ (**2**)[24, 25] has two inequivalent carbonate ligand environments and should give rise to two, equal intensity resonances as seen in Figure 1 at pH 6.0. The observed ^{13}C NMR data is consistent with this structure proposed by Ciavatta *et al.*[24]

The chemical shift difference between the two carbonate signals indicates that the two carbonate carbon environments are very different. Since the monomer (**1**) has only terminal carbonate ligands which are observed at δ 165.2 ppm, this establishes the chemical shift region for the terminal ligands of the system. For the trimer (**2**) the low frequency resonance at δ 164.9 ppm can be assigned to the terminal carbonate ligand, and the high frequency resonance at δ = 166.2 ppm to the bridging carbonate ligand. The integrated NMR resonances appear in a 1:1 bridge:terminal ratio. Cooling the sample results in a substantial decrease in the line-width of the high field signal as shown in Figure 1b. This is further indication that the resonance at δ 164.9 is due to a terminal ligand since carbonate ligand exchange is expected to be more facile for a terminal ligand than a bridging ligand.[27]

Commensurate with the slowed exchange process at 0 °C, free bicarbonate and CO_2 are observed. Thus the exchange between free carbonate in solution and the terminal carbonate ligands in the uranyl carbonate complexes causes the line-broadening in the terminal carbonate resonance. A more detailed set of experiments was performed for a 0.05 *M* uranyl sample with an ionic strength of 2.5m in order to determine the thermodynamic equilibrium constant. The longitudinal relaxation rate (T_1) was measured using the inversion recovery method to be 35.9 s, and a 180 s ($5T_1$) pre-acquisition delay was used to obtain accurate integration data. A ^{13}C NMR titration of this sample performed at 0 °C was examined for determination of an equilibrium constant, and a portion of this NMR titration is shown in Figure 2.

^{17}O NMR. Once the conditions that favored monomer and trimer formation were established by ^{13}C NMR, we sought to examine the solution species in further detail using ^{17}O NMR spectroscopy, and to compare our results with the original ^{17}O data.[38] The integrated intensities of ^{17}O NMR resonances are generally only a qualitative measure of relative numbers of oxygen nuclei; however, intensity data are quite reliable when the resonances being compared have similar linewidths and chemical shifts.[40,41]

Our first objective was to establish the chemical shift region for the uranyl and carbonate oxygen atoms in the ^{17}O NMR spectra of the individual components. ^{17}O-enriched samples of the uranyl ions were prepared electrochemically, and carbonate solutions were prepared in a bomb reactor, as described in the experimental section. The ^{17}O NMR spectrum (33.9 MHz) for ^{17}O-enriched HCO_3^- at pH 8.3 shows a single, broad ($\Delta\nu_{1/2}$ = 400 Hz) resonance at δ 175 ppm, and a sample at pH 10.97 shows a resonance at 190.9 ppm ($\Delta\nu_{1/2}$ = 420 Hz). This compares favorably to the value of δ 192 ppm observed for the CO_3^{2-} ion in 0.1*M* KOH solution.[39] Since the chemical shift is a weighted average of CO_3^{2-} and HCO_3^- chemical shifts, its position will be sensitive to pH. The broad linewidth of the HCO_3^- ion ($\Delta\nu_{1/2}$ = 400 Hz) may be a result of CO_3^{2-} + HCO_3^- chemical exchange. The observed chemical shift range of 175 - 190 ppm is in accord with the so-called "double-bond rule" in which chemical shifts are assumed to depend linearly on π bond order.[41] For example, aldehydes and ketones (π bond order of 1) are observed near δ 600 ppm, and this implies a chemical shift of about 200 for pure CO_3^{2-} (π bond order of 1/3).[41] The ^{17}O NMR spectrum of the UO_2^{2+} ion in 1*M* $HClO_4$ revealed a chemical shift of δ 1121 ppm, and can be compared to δ 1119 ppm reported by Fukutomi *et al.*[42,43]

An ^{17}O NMR spectrum of a sample of ^{17}O-enriched monomeric $U^*O_2(C^*O_3)_3^{4-}$ (**1**) recorded at pH 9.7 revealed a uranyl oxygen in the expected chemical shift region at δ 1098 ppm, and two other oxygen resonances in the carbonate oxygen region at δ 225 and 185 ppm, shown in Figure 3. The uranyl oxygen resonance at δ 1098 is relatively sharp ($\Delta\nu_{1/2}$ = 6 Hz) as expected. Both resonances in the carbonate chemical shift region are very broad, indicative of chemical exchange. The resonance at δ 185 ppm is consistent with free carbonate + bicarbonate ions at pH 9.7. The other broad resonance at δ 225 ppm is consistent with carbonate ligands in the coordination sphere of the uranyl ion.

The carbonate oxygen resonances seen at δ 185 and 225 at pH 9.7 (Figure 3) undergo coalescence when the pH is lowered below 9. This is undoubtedly a result of an increase in the rate of carbonate ligand exchange with increasing hydrogen ion concentration. Examination of this

system at a higher field strength (67.8 MHz) did not result in "freezing out" the chemical exchange of the carbonate ligands. Thus the carbonate oxygen resonances were never observed in this study below pH 9. The uranyl oxygen resonances remain sharp as the pH is lowered, as these oxygen atoms do not exchange on the NMR timescale. The uranyl oxygen region of the ^{17}O NMR spectra at 0 °C as a function of pH is extremely informative and is shown in Figure 4 (33.9 MHz). At pH 7.87, there is a single uranyl-containing species with a resonance at δ 1098 ppm. We have already established that this resonance is attributed to monomeric $UO_2(CO_3)_3^{4-}$. As the pH is decreased, a second uranyl oxygen resonance appears at δ 1105 ppm. The resonance due to $UO_2(CO_3)_3^{4-}$ decreases while the new resonance assigned to the equivalent uranyl oxygen atoms in $(UO_2)_3(CO_3)_6^{6-}$ increases, until, at pH 6.0, the trimer, **2**, is the predominant uranyl-containing species in solution.

The NMR data amassed thus far are consistent with two observable species under the conditions employed in this study. The ^{13}C and ^{17}O NMR data are consistent with the formation of trimeric $(UO_2)_3(CO_3)_6^{6-}$ as proposed by Åberg *et al.*[25] However, we admit that the ^{13}C and ^{17}O NMR resonances are equally consistent with formation of a dimer of formula $(UO_2)_2(CO_3)_4^{4-}$ (i.e. one bridge and one terminal ligand). For this reason, we examined this system using vibrational spectroscopy, Extended X-ray Absorption Fine Structure (EXAFS), and x-ray diffraction to get more definitive information regarding the structure in solution and the solid state.

Solid Samples. Solution NMR studies and the thermodynamic data of Grenthe revealed the conditions under which solutions of a single component could be prepared reproducibly. This allowed for the preparation of samples that contained nearly pure monomeric $UO_2(CO_3)_3^{4-}$ or trimeric $(UO_2)_3(CO_3)_6^{6-}$ anions. Counter cations were added to the trimer solutions, followed by slow cooling to 5 °C under a CO_2 atmosphere, in multiple attempts to isolate crystalline samples suitable for X-ray diffraction studies. Either amorphous or microcrystalline precipitates, or clear yellow solutions were obtained using Na^+, K^+, Me_4N^+, Et_4N^+, n-Pr_4N^+, and Ph_3MeN^+ counter

cations. We also examined the use of cryptands (Kryptofix 222, Kryptofix 211) or crown ethers (18-crown-6) in the presence of Na^+ or K^+ ions. None of these attempts provided crystalline samples. In contrast, the guanidinium cation $C(NH_2)_3^+$ yielded single crystals of compounds of empirical formula $[C(NH_2)_3]_4[UO_2(CO_3)_3]$ (**3**) and $[C(NH_2)_3]_2[UO_2(CO_3)_2]$ (**4**) based on combustion elemental analysis. Monomeric $[C(NH_2)_3]_4[UO_2(CO_3)_3]$ crystals were suitable for single crystal x-ray diffraction, while trimeric $[C(NH_2)_3]_6[UO_2(CO_3)_2]_3$ formed small, thin plates that were unsuitable for single crystal x-ray diffraction studies. However, the use of stoichiometric amounts of uranyl nitrate and guanidinium carbonate followed by the addition of two equivalents of guanidinium nitrate produced crystals of formula $[C(NH_2)_3]_6[(UO_2)_3(CO_3)_6]\cdot 6.5H_2O$ (**5**) which were suitable for single crystal x-ray diffraction.

Vibrational Spectroscopy. Infrared spectra of crystalline samples of $[CN_3H_6]_4[UO_2(CO_3)_3]$, $[CN_3H_6]_6[(UO_2)_3(CO_3)_6]$, and $[C(NH_2)_3]_6[(UO_2)_3(CO_3)_6]\cdot 6.5H_2O$ (Nujol mull and KBr pellet) showed vibrational bands characteristic of guanidinium ions, as well as characteristic group vibrational frequencies (ν_1, ν_2, ν_3, ν_4) for the carbonate ligand. It is well established that the carbonate ν_3 vibration is split into two components upon coordination to a metal ion.[44] This splitting is generally on the order of 50 - 60 cm^{-1} for monodentate and 160 - 190 cm^{-1} for bidentate coordination.[44] The splitting of the ν_3 mode by 181, 145, and 159 cm^{-1} (KBr) in crystalline samples of **3**, **4**, and **5** (respectively) is consistent with bidentate or bridging carbonate ligands. A resolved peak for the asymmetric O=U=O stretch was not observed in any guanidinium salt of the uranyl compounds. While the spectrum of **5** had an unresolved shoulder in the 915 cm^{-1} region, the uranyl peak was "masked" by the strong ν_2 carbonate out-of-plane deformation at 894, 895, and 892 cm^{-1} in **3**, **4**, and **5** respectively. However, a well-known relationship between Raman active (ν_1) and IR active (ν_3) O=U=O stretching modes allows for a calculation of the uranyl (ν_3) at 889 and 911 cm^{-1} from Raman data for the **3** and **4** respectively.[45]

Solution Raman spectra recorded on samples containing pure $UO_2(CO_3)_3^{4-}$ at pH 8.0 showed the symmetric ν_1 O=U=O stretch at 812.5 cm^{-1}, while Raman spectra of a sample containing pure $(UO_2)_3(CO_3)_6^{6-}$ at pH 6.0 showed a significant shift in the ν_1 O=U=O stretch to 831.6 cm^{-1}. The axial O=U=O force constant can be estimated to within 3% from the symmetric O=U=O stretching band ν_1 (Raman active) and the asymmetric ν_3 (IR active) using the equation $k = 4.713 \times 10^{-6} (\nu_1^2 + (\nu_3^2 / 1.314))$, where k is the force constant in mdyne/Å and ν is in cm^{-1}.[46] For the monomeric species, with ν_1 = 812.5 cm^{-1} and ν_3 = 911 cm^{-1}, k = 6.088 mdyne/Å; for the trimeric species, with ν_1 = 831.6 cm^{-1} and ν_3 =889 cm^{-1}, k = 6.094 mdyne/Å. Therefore, the uranyl bond for the trimer is somewhat stronger than the monomer. The explanation of uranyl bond strength differences has been traditionally attributed to the strength of the equatorial bonding.[45] Specifically, ligand-to-metal σ- and π-bonding of the equatorial ligands pushes electron density towards the uranium metal center and increases electrostatic repulsion with the highly negative axial oxygen atoms to weaken the bonds. Therefore, weaker $U=O_{ax}$ bonds imply stronger equatorial bonding by carbonate ligands in the monomer (3 carbonates per U) than the trimer (2 carbonates per U). Finally, application of a modified Badger's rule, as used by previous workers[46-49] through the equation ($r = 1.08\ k^{-1/3} + 1.17$) gives an axial U=O bond length of approximately 1.75 Å for both monomer and trimer. Note that this equation shows that vibrational frequencies are much more sensitive indicators for bond strengths than bond lengths.

EXAFS Studies. Single crystals of $[C(NH_2)_3]_6[(UO_2)_3(CO_3)_6]$ formed as extremely thin plates that were unsuitable for single crystal x-ray diffraction analysis. Therefore, we investigated the structure of $[C(NH_2)_3]_6[(UO_2)_3(CO_3)_6]$ by Extended X-ray Absorption Fine Structure (EXAFS) spectroscopy. In particular, a comparison of $[C(NH_2)_3]_6[(UO_2)_3(CO_3)_6]$ with a monomeric $M_4[UO_2(CO_3)_3]$ would confirm the presence of an oligomeric species if a U-U backscattering interaction was observed in the former. X-ray absorption measurements were performed at the uranium L_{III}-edge for three species, solid $[C(NH_2)_3]_6[(UO_2)_3(CO_3)_6]$, solid

$K_4[UO_2(CO_3)_3]$, and a 0.2 *M* aqueous solution of ^{13}C-enriched $(UO_2)_3(CO_3)_6^{6-}$ at pH 5.7 under 1 atmosphere of CO_2. ^{13}C NMR spectra of this solution were examined both before and after EXAFS analysis, and indicated that $(UO_2)_3(CO_3)_6^{6-}$ was present in excess of 99% based on NMR integration, and that X-ray exposure did not cause significant sample degradation. The theoretical EXAFS modeling code, FEFF6, of Rehr *et al.*[50,51] was employed to calculate the backscattering phases and amplitudes of the individual neighboring atoms, using the proposed structure **2** as a structural model.

Solid $[C(NH_2)_3]_6[(UO_2)_3(CO_3)_6]$ (4). Figure 5 shows the raw background-subtracted EXAFS spectrum and its Fourier transform for solid $[C(NH_2)_3]_6[(UO_2)_3(CO_3)_6]$. The Fourier transform reveals five well resolved peaks, labeled A-E in Figure 5(b). The peaks occur at lower R values with respect to their true atomic positions due to the EXAFS phase shift ($\alpha \sim 0.2$-0.5 Å). Qualitative assignment of these peaks in terms of the model trimeric structure **2** is straightforward, with the exception of peak C. Peak A corresponds to the uranyl oxygens, while the asymmetric peak B arises from the six carbonate oxygens (bidentate ligation) in the equatorial plane together with the carbonate carbon atoms. The terminal oxygens of the carbonate groups give rise to peak D. The small peak at ca. 4.75 Å (E) may, at this level, be tentatively assigned to backscattering from the other uranium atoms of the trimeric unit.

Fitting of the experimental data on the basis of the preceding discussion is hampered by the existence of peak C, which at ca. 3.5 Å does not correspond to any single uranium-backscatterer distance in $UO_2(CO_3)_3^{4-}$ or in $(UO_2)_3(CO_3)_6^{6-}$. One possible source to consider for this interaction may be multiple scattering associated with the linear uranyl subunit. Multiple scattering is a well established phenomenon in EXAFS spectroscopy,[52-55] and contributes significantly when two or more atoms surrounding the photoabsorber are collinear. In this case peak C lies at an R value which is approximately twice that of peak A, suggesting multiple scattering along the uranyl vector as its origin. We have observed a similar peak in the Fourier transforms of the

EXAFS for a variety of uranyl-containing compounds, including aqueous solutions of UO_2Cl_2.[56] Further support for this assertion is provided by FEFF6, which calculates a uranyl multiple scattering pathway with an effective R value twice the uranyl U-O distance. This path is calculated to have an amplitude ratio which is ~21 % of the single scattering uranyl path. Additional theoretical modeling with FEFF6 reveals that multiple scattering effects are also significant for the terminal oxygens from the carbonates and the uranium neighbors in the trimer. In each case, a linear configuration exists (i.e., U—C—O and U—O—U), and multiple-scattering pathways along these units contribute significantly to the EXAFS Fourier transform peaks D and E, respectively. As a result, curve fits were performed using FEFF6 to model single scattering pathways for peaks A and B and multiple scattering pathways for peaks C, D, and E.

Figure 5 shows the best fit obtained using this approach and the fit parameters are given in Table I. The fit quality is generally very good. Table II shows typical metrical parameters for the $UO_2(CO_3)_3^{4-}$ from the literature.[10,57] Comparison of Tables I and II shows that the fitted EXAFS distances for $[C(NH_2)_3]_6[(UO_2)_3(CO_3)_6]$ agree very closely with the X-ray crystallographic data for $Na_2Ca[UO_2(CO_3)_3].xH_2O$ ($x \approx 5.6$)[10] and $K_4[UO_2(CO_3)_3]$.[57]

The most important result is the existence of peak E, whose EXAFS frequency and phase shift are characteristic of a U-U interaction at a distance of 4.91 Å. The EXAFS results are therefore consistent with an oligomeric structure for the uranium-containing component of $[C(NH_2)_3]_6[(UO_2)_3(CO_3)_6]$. However, due to the correlation between the coordination number and the Debye-Waller factor in fitting the EXAFS amplitude, the uncertainty in the U coordination number is such that EXAFS is unable to distinguish between a dimeric and a trimeric structure.

Aqueous $[(UO_2)_3(CO_3)_6]^{6-}$ (2). In order to obtain a more direct comparison with the NMR experiments, the EXAFS of the $[(UO_2)_3(CO_3)_6]^{6-}$-containing uranyl carbonate solution was investigated. Figure 6 shows the EXAFS spectrum and its Fourier transform. The data are nearly identical to those of the solid compound (Figure 5), with five well resolved peaks in the

transform, suggesting that the same species are present in both the solid and solution. In particular, the observation of peak E in the Fourier transform of the solution EXAFS lends further weight to the NMR evidence by supporting an oligomeric structure.

The experimental EXAFS was fitted using the same approach as for $[C(NH_2)_3]_6[(UO_2)_3(CO_3)_6]$. The results are given in Table I. As before, the fit is very good. Once again we are unable to distinguish between a dimeric and a trimeric structure, but the EXAFS results are entirely consistent with the presence of an oligomeric species with a U-U distance of 4.92 Å.

Solid $K_4[UO_2(CO_3)_3]$. In order to verify the origin of the phase-shifted peak at 4.75 Å in the Fourier transforms of both $[C(NH_2)_3]_6[(UO_2)_3(CO_3)_6]$ and the $[(UO_2)_3(CO_3)_6]^{6-}$-containing uranyl carbonate solution, we investigated the EXAFS for solid $K_4[UO_2(CO_3)_3]$. This monomeric compound should display EXAFS which is similar to that of the trimeric species but which has no U-U backscattering contribution. Figure 7 shows the EXAFS spectrum and its Fourier transform, both of which are quite similar to their counterparts in Figures 5 and 6. Closer inspection reveals some subtle differences in the Fourier transform of the monomer. That is, the uranyl multiple scattering resonance appears to be more intense and has shifted to higher R, and peak B appears to be sharper with a shoulder now on the high R side. Of key importance, however, is the absence of any peak beyond an R value of 4.0 Å, which provides further evidence to support the oligomeric nature of the uranium-containing species in both $[C(NH_2)_3]_6[(UO_2)_3(CO_3)_6]$ and the uranyl carbonate solution.

The experimental data were fit with the FEFF6 phases and amplitudes described previously for the trimeric compounds, however, with two important changes to the model. In this case, the U-U interaction was not included since it is apparently not observed in the raw EXAFS Fourier transform. In addition, examination of the crystal data for $K_4[UO_2(CO_3)_3]$ reveals that six K atoms lie at ca. 3.81-3.85 Å from the central U. As a result, a shell of K atoms (using single scattering) was included in the fit. This latter contribution gives rise to a more complicated

interference pattern in the monomer Fourier transform and helps to explain its different appearance with respect to the Fourier transforms of the trimeric compounds. The fitting results are given in Table I. The agreement between the experimental and fitted Fourier transforms is very good. The results on $K_4[UO_2(CO_3)_3]$ reinforce the conclusions drawn from the data on $[C(NH_2)_3]_6[(UO_2)_3(CO_3)_6]$ and the uranyl carbonate solution, and support the assertion that they contain oligomeric uranyl carbonate species.

Single Crystal X-ray Diffraction Studies

$[CN_3H_6]_6[(UO_2)_3(CO_3)_6]\cdot 6.5H_2O$. X-ray quality crystals of **5** were grown by slow cooling of a concentrated aqueous solution containing excess guanidinium nitrate to 5 °C under a CO_2 atmosphere, and the structure was determined from diffraction data collected at -44 °C. Data collection and crystallographic parameters are summarized in Table III. Selected fractional coordinates for the $(UO_2)_3(CO_3)_6^{6-}$ anionic unit are given in Table IV and selected bond lengths and angles for the $(UO_2)_3(CO_3)_6^{6-}$ unit are given in Table V. An ORTEP drawing giving the atom-numbering scheme used in the tables is shown in Figure 8. The solid state molecular structure of $[C(NH_2)_3]_6[(UO_2)_3(CO_3)_6]\cdot 6.5H_2O$ contains six guanidinium cations, 6.5 H_2O molecules, and a planar D_{3h} trimetallic $(UO_2)_3(CO_3)_6^{6-}$ cluster anion, which are all involved in hydrogen bonding. The trimetallic cluster anion contains three uranium atoms and all six carbonate ligands within a molecular plane. Three uranyl oxygen atoms lie above, and three lie below the molecular plane. Uranyl O=U=O angles average 179.1(6) degrees with an average U=O distance of 1.78(1)Å. This distance can be compared with the 1.75Å determined from vibrational spectroscopy, and the 1.79Å determined by EXAFS spectroscopy. This distance is comparable to the uranyl distances found in other uranyl containing solids, and the distances of 1.80(2), 1.802(6), 1.79(1), 1.78(2), and 1.76(2)Å found in the solid state structures of $Na_2Ca[UO_2(CO_3)_3]\cdot 5.6H_2O$,[10] $K_4UO_2(CO_3)_3$,[57] $(NH_4)_4UO_2(CO_3)_3$,[29] $(CN_3H_6)_4[UO_2)(O_2)(CO_3)_2]\cdot 2H_2O$,[58] and $(CN_3H_6)_4[(UO_2)_2(C_4H_6N_2O_2)(CO_3)_3]\cdot H_2O$,[59]

respectively. U-O distances to the carbonate ligands average 2.41(1)Å for terminal ligands, while bridging carbonates have somewhat longer distances of 2.48(1)Å (ave). The terminal U-O carbonate distances are comparable to other terminal bidentate distances such as 2.44(1) and 2.430(5)Å seen in $Na_2CaUO_2(CO_3)_4 \cdot 5.6\ H_2O$,[10] and $K_4UO_2(CO_3)_4$,[57] respectively. To the best of our knowledge, the only other example of a bridging carbonate ligand between uranyl centers is in the solid state structure of the dioximato complex $(CN_3H_6)_4[(UO_2)_2(C_4H_6N_2O_2)(CO_3)_3] \cdot H_2O$.[59] The latter compound shows a distinct asymmetry in the bridging carbonate ligand in that the "internal" U-O distance is 2.38(1) while the four "external" U-O bonds average 2.53(2) Å.[59] We do not see any similar asymmetries in our data. However, we do see statistically significant differences in the C-O bonds and O-C-O angles of the carbonate ligands. Terminal carbonate C-O bonds average 1.27(2) Å, and O-C-O angles average 114.0(16) and 123.0(16)°, with the more smaller angle lying between oxygen atoms bound to the uranium centers. The bridging carbonate ligands show a significant asymmetry in C-O bond lengths. Internal C-O bond lengths [C(1)-O(1); C(2)-O(4); C(3)-O(7)] average 1.33(2), while the six external C-O bonds average 1.26(2)Å. Likewise, the six internal O-C-O angles average 116.5(15)°, while the three external angles average 127.0(15)°. For the bridging carbonate ligands, the U-O-U angle for the internal oxygen atoms [O(1), O(4), O(7)] are nearly linear and average 170.7(6)°. Particularly significant is the average nonbonding U--U distance of 4.967(1) Å, which compares favorably to the 4.91 Å distance seen in the EXAFS analysis. A comparison of metrical parameters derived from EXAFS and X-ray diffraction data is given in Table VI. The agreement is excellent.

A ball-and-stick drawing illustrating the three dimensional packing and hydrogen bonding of $C(NH_2)_3^+$ and $(UO_2)_3(CO_3)_6^{6-}$ ions, and H_2O molecules within the unit cell is shown in Figure 9. The planar guanidinium ions show average C-N distances of 1.32(2)Å. Both guanidinium cations and water molecules are involved in strong hydrogen bonding interactions to the $(UO_2)_3(CO_3)_6^{6-}$ anion. These interactions are quite strong as evidenced by short O--O contacts

between water molecules and terminal or bridging carbonate oxygen atoms, which average 2.648(20) and 2.771(20) Å, respectively. In a similar fashion, short O--N contacts are observed between guanidinium nitrogen atoms and terminal or bridging carbonate oxygen atoms averaging 2.750(14) and 2.819(20) Å, respectively.

Analysis of Solution Thermodynamic Data

General considerations. The EXAFS and X-ray diffraction studies have verified that trimeric $(UO_2)_3(CO_3)_6^{6-}$ is the predominant solution species at pH 6.0 under our experimental conditions of $[UO_2^{2+}] = 0.05M$, and $[CO_3^{2-} + HCO_3^-] = 0.15M$. Therefore, the ^{13}C NMR integrations can be used to measure the monomer and trimer concentrations for a determination of the equilibrium constant for comparison with published thermodynamic data.[7] The published data have generally been measured under different conditions and need to be converted to a standard thermodynamic state to make meaningful comparisons. Secondly, an accurate determination of the hydrogen ion concentration was necessary.

Hydrogen ion concentration; p[H]. To evaluate proton dependent thermodynamic data, it is important to know $-\log[H^+]$ with high accuracy and precision.[60-62] Using the accepted equilibrium constants (Table VII) for the reactions shown in eqs 2-4,[7] one can calculate p[H][62] as a function of ionic strength using specific ion interaction theory and tabulated coefficients.[7] High ionic strength (2.5 and 3.0 m) buffer solutions were prepared by equilibrating solutions of $NaClO_4 \cdot H_2O$ and $NaHCO_3$ with CO_2 gas mixtures of known compositions (Experimental section). The pH electrode was calibrated using commercial pH buffer solutions, and then pH readings of our synthetic buffers were recorded after 48, 72, and 120 hrs, and found to be stable. This calibration gives p[H] values, and at these ionic strengths, pH and p[H] values can differ by as much as 0.6 log units (Experimental section).

$$CO_3^{2-} + H^+ \rightleftharpoons HCO_3^- \quad (2)$$

$$CO_3^{2-} + 2\,H^+ \rightleftharpoons CO_2\,(aq) + H_2O \quad (3)$$

$$H^+ + HCO_3^- \rightleftharpoons CO_2\,(g) + H_2O \quad (4)$$

Thermodynamic Equilibrium Constants. One purpose of this study was to evaluate the applicability of multinuclear NMR spectroscopy as a *species-specific* probe to track relative concentrations (species distributions) of actinide carbonate complexes as a function of -log[H^+]. The distribution of species observed by multinuclear NMR can be compared with predictions based on data recorded under other conditions. In order to understand and model the total system, we considered hydrolysis, carbonate complexation, and carbonate/bicarbonate equilibria. Log equilibrium quotients at zero ionic strength for hydrolyzed uranyl species were taken from the recently published review of uranium data.[7] The solubility product for $UO_2(OH)_2$ (s) was taken from Baes and Mesmer.[63] All the log equilibrium quotients used in our calculations are given in Table VII (species other than those listed in the tables were not considered).

All of the log equilibrium quotients (log β's) were corrected for ionic strength using the Specific ion Interaction Theory (SIT) according to eq 5.[7] In eq 5, I_m is the ionic strength in molality, Δz^2 is the difference in the sum of the squares of the ionic charges, and $\Delta\varepsilon$ is similarly defined in terms of the change in appropriate specific interaction coefficients, and n is the number of water molecules. The quantities β^m, and β^0 represent the formation constant of a complex in an ionic medium (β^m) or corrected to an ionic strength of zero (β^0). The log of the activity of water ($\log_{10} a_w$) is given by equation 6, where Φ is the osmotic coefficient of the solution. The osmotic coefficients were estimated to be the same as for $NaClO_4$ as given in Robinson and Stokes.[64] Quadratic equations for Φ as a function of concentration were fit to two concentration regions: 0.4 m ≤ I_m ≤ 1.0 m, and 1.0 m ≤ I_m ≤ 4.0 m. The interaction coefficients used are from the uranium thermodynamic review.[7]

$$\log_{10} \beta^m = \log_{10} \beta^0 + \Delta z^2 \left(\frac{0.5091\sqrt{I_m}}{1 + 1.5\sqrt{I_m}} \right) - \Delta\varepsilon(I_m) + n \log_{10} a_w \quad (5)$$

$$n \log_{10} a_w = \frac{-2m\Phi}{\ln(10) \times 55.51} \quad (6)$$

Five determinations for the formation of the trimeric $(UO_2)_3(CO_3)_6^{6-}$ complex, $\log\beta_{36}$, were reviewed by the Nuclear Energy Agency (NEA) for the reaction shown in equation 7. Those determinations were not consistent, and the NEA review selected the unweighted average of these values to be $\log\beta^0_{36} = 54.0 \pm 1.0$.[7] The direct observation of this species by multinuclear NMR provides the opportunity to refine this value. In our NMR experiments, the experimental observables were those indicated in equation 8, and hence we cannot determine $\log\beta_{36}$ directly. Quantitative ^{13}C NMR experiments were performed for a 0.05 *M* uranyl sample with an ionic strength of 2.5m in order to examine the equilibrium constant for the reaction shown in equation 8. Accurate NMR integrations were possible in the range of p[H] between 7.3 - 7.7. At p[H] lower than 7.3, CO_2 had to be placed over the solution to stabilize the p[H], hence the carbonate concentration could not be known accurately. The four measurements obtained in this range give logK = 18.1(±0.5) at 2.5m ionic strength and 25°C for equation 8. We used Specific Ion Interaction theory, and the interaction coefficients recommended by the NEA to calculate the equilibrium constants for reactions 2-4 and 9 at 2.5m ionic strength. These values are indicated in Table VII. These values were then used to calculate $\log\beta_{36} = 55.6(\pm0.5)$ for equation 7 at 2.5m and 25°C. This value can be compared with the calculated value from the NEA review at 2.5m (Table VII) of $\log\beta_{36} = 55.32(\pm1.0)$. The agreement is excellent.

$$3\ UO_2^{2+} + 6\ CO_3^{2-} \rightleftharpoons (UO_2)_3(CO_3)_6^{6-} \quad (7)$$

$$3\ UO_2(CO_3)_3^{4-} + 3\ H^+ \rightleftharpoons (UO_2)_3(CO_3)_6^{6-} + 3\ HCO_3^- \quad (8)$$

$$UO_2^{2+} + 3\ CO_3^{2-} \rightleftharpoons UO_2(CO_3)_3^{4-} \quad (9)$$

Concluding Remarks

The ^{13}C and ^{17}O NMR, IR, and Raman experiments are consistent with the formation of $(UO_2)_3(CO_3)_6^{6-}$, as originally proposed by Ciavatta *et al.*[17] EXAFS data from solid $[C(NH_2)_3]_6[(UO_2)_3(CO_3)_6]$ and a solution of $(UO_2)_3(CO_3)_6^{6-}$ suggest that the same uranium species is present in both the solid and solution states. Fourier transforms of the EXAFS spectra of both solid and solution samples revealed 5 well-resolved peaks corresponding to U=O = 1.79, U-O (carbonate) = 2.45, U--C = 2.90, U--O (carbonate) = 4.16 and U--U- 4.91 Å for the solid, and similar distances for the solution sample. The peak at 4.75 Å in both Fourier transforms (uncorrected for phase shift) corresponds to the U--U interaction at 4.91 Å, a conclusion which is supported by the absence of the peak in the Fourier transform of crystalline monomeric $K_4[UO_2(CO_3)_3]$. Multiple scattering along the uranyl vector is believed to play a significant role in the EXAFS of all three systems. The EXAFS data are consistent with the trimeric uranyl carbonate species indicated by NMR spectroscopy. The solid state molecular structure of $[C(NH_2)_3]_6[(UO_2)_3(CO_3)_6]\cdot 6.5H_2O$ confirms a planar D_{3h} trimetallic $(UO_2)_3(CO_3)_6^{6-}$ anion as originally proposed by Åberg *et al.*[25] Particularly significant is the average nonbonding U--U distance of 4.97 Å which compares favorably to the 4.91 Å distance seen in the EXAFS spectrum. The NMR data allows for the determination of $\log\beta_{36} = 55.6(\pm 0.5)$ at 2.5m and 25°C, which is in excellent agreement with the value recommended by the NEA.[7]

These ^{13}C and ^{17}O NMR studies demonstrate the utility of multinuclear NMR as a *species-specific* probe for actinide solution studies. Other, more traditional approaches to speciation require that potentiometric, coulombic, solubility, or absorption spectrophotometric data be fit to a numerical model and refined using nonlinear least-squares analysis. The commonly used method for measurement and refinement of equilibrium constants is still potentiometric titration followed by curve-fitting a set of thermodynamic constants to the data. However, in some cases so many species have been used to fit the observed data such that the resulting parameters are questionable, or unreasonable species are included in the model. The problems of low-quality fits and putative

species makes it desirable to have alternate methods available with which to validate the species and their corresponding thermodynamic constants. The multinuclear NMR approach allows for direct observation of different species, thereby removing some ambiguity in assigning relevant species to explain solution data. Concentrations are measured from the data by integration, and thermodynamic equilibrium constants can be calculated. This work also demonstrates that multinuclear NMR spectroscopy will be a valuable *species-specific* tool for determining new equilibria and equilibrium constants for transuranium complexes.

Uranium(VI) is by far the most well-studied actinide system available, and the reviewers of the uranium(VI) literature[7] appear to have done an outstanding job of critically analyzing this data and suggesting a suitable set of thermodynamic constants for hydrolysis and carbonate complexation of uranium(VI). This NMR study validates a subset of these thermodynamic constants. Future multinuclear NMR studies of the important transuranic systems will provide insight for choosing the best model to fit new and existing thermodynamic data. This multiple method approach should provide the most accurate estimate of thermodynamic constants for use in geochemical, site assessment, and performance assessment modeling. Further studies of An(VI) and An(V) (An = Np, Pu, Am) carbonate complexation by multinuclear NMR, EXAFS, and X-ray diffraction are in progress.

Experimental

General considerations. All manipulations were carried out inside fume hoods or negative pressure gloveboxes designed for containment of radioactive materials in a laboratory equipped with appropriate safeguards for manipulation of such materials (monitoring devices, HEPA-filtered ventilation, etc.). Standard radiochemical procedures were used throughout. Ultra-pure $HClO_4$, "Supra-pure" NaOH, and sodium perchlorate monohydrate (Fluka) were used without purification. Sodium carbonate, sodium bicarbonate, and guanidine carbonate (Aldrich)

were used without further purification. Guanidinium nitrate was prepared from guanidine carbonate and nitric acid. D_2O (99.9% D) and ^{13}C-enriched Na_2CO_3 (99.9% ^{13}C) were purchased from Cambridge Isotopes. Deuterium oxide was degassed by bubbling with argon for 1 hr, and the $Na_2{}^{13}CO_3$ was used as received. ^{17}O-enriched H_2O (20% ^{17}O) was obtained from Los Alamos National Laboratory Stock, and used without further purification. $UO_2(ClO_4)_2(H_2O)_6$ was recrystallized 3 times from perchloric acid. pH was measured using a Corning model 130 pH meter and an ORION (ROSS, model 8103) combination electrode. Carbon dioxide gas was humidified by bubbling through a 3.0 *M* KCl solution prior to passing over samples in order to maintain a constant vapor pressure and minimize evaporation of sample solutions.

Solution UV-visible-NIR spectra were recorded using a Perkin-Elmer Lambda 9 Spectrophotometer and matched 1.0 or 0.1 cm quartz cells. Electrochemical syntheses of ^{17}O-labeled actinide solutions were performed using an EG&G PARR Model 173 potentiostat/coulometer. Electrochemical cells used for bulk electrolysis had separate compartments for reference and counter-electrodes and are described in detail elsewhere.[65] A Pt screen working electrode was separated from a Pt wire counter electrode by a Vicor frit, and a saturated calomel electrode (SCE) was used as a reference electrode. Elemental analyses were performed on a Perkin-Elmer 2400 CHN analyzer. Infrared spectra were recorded as KBr pellets, or as Nujol mulls between KBr plates on a Digilab FTS-40 spectrometer. Elemental analysis samples were prepared and sealed in tin capsules in the glovebox prior to combustion.

All NMR sample solutions were loaded into Wilmad 5mm o.d. 507-PP Pyrex glass NMR tubes which were flame-sealed with a small hand torch. Variable-temperature FT ^{13}C and ^{17}O NMR spectra were recorded on a Bruker AF 250 spectrometer fitted with a 5mm broadband probe operating at 62.9 (^{13}C) or 33.9 (^{17}O) MHz, or on a Varian Unity 300 spectrometer with a 5mm broadband probe operating at 75.4 (^{13}C) or 40.7 (^{17}O) MHz, or on a Bruker AMX500 spectrometer with a 5mm broadband probe operating at 67.8 (^{17}O) MHz with ^{2}H field-frequency lock. The ^{13}C $\pi/2$ pulse length was measured to be 5.25 (62.9 MHz) and 17.0 μs (75.4 MHz)

using the free carbonate resonance. The ^{17}O $\pi/2$ pulse length was measured to be 11.8 (33.9 MHz) and 13.8 μs (67.8 MHz) using the free water resonance. The temperature was controlled with Bruker or Varian variable temperature controllers and was stable to within ±1K. The temperature was determined by measurement of the ^{1}H NMR of ethylene glycol (295 - 350 K) or methanol (270 -295 K) at the same temperature and gas flow rate. All ^{13}C NMR chemical shifts are reported in ppm relative to the carbonyl carbon of external acetone-d_6 set at $\delta = 206.0$. All ^{17}O NMR chemical shifts are reported in ppm relative to external H_2O set at $\delta = 0$.

Preparation of bicarbonate p[H] buffers. Buffer solutions were prepared by equilibrating solutions of $NaClO_4$ and $NaHCO_3$ with CO_2 gas mixtures of known compositions. All buffers were transferred to gas scrubbers and saturated with the appropriate gas mixtures. An Orion Ross Combination electrode was calibrated with commercial buffers at pH=7 and pH=10 on an Orion ion analyzer, and then pH readings of our bicarbonate pH buffers were recorded after 48, 72, and 120 hrs and found to be stable. Density readings for each synthetic buffer were obtained by weighting 10 mL of each solution. A barometric pressure of 570 mm Hg (7,300 ft above sea level) was used.

Ionic strength 3.0 m. p[H] was plotted against pH and linear regression gave the following pH correction for experiments at an ionic strength $I_m = 3.0$ molal. p[H] = 1.00828(pH) + 0.520468, $R^2 = 0.9996$. Buffer #1, p[H] 8.70. 27.34 mL of 8.93M $NaClO_4$ solution (244.15 mmol), and 1.6803 g (20.00 mmol) of $NaHCO_3$ were combined and dissolved with 100 mL distilled water in a volumetric flask to give a solution of composition 2.4415 M $NaClO_4$, 0.2 M $NaHCO_3$, $\rho = 1.2013$ g/mL, and I = 3.00 molal. This solution was bubbled with 3% (f-CO_2 = 0.03) CO_2-Ar to establish equilibrium. Buffer #2, p[H] 7.76. 27.34 mL of 8.93 M $NaClO_4$ solution (244.15 mmol), and 1.6818 g (20.02 mmol) of $NaHCO_3$ were combined and dissolved with 100 mL distilled water in a volumetric flask to give a solution of composition 2.4415 M

$NaClO_4$, 0.2002 M $NaHCO_3$, ρ = 1.2039 g/mL, and I = 2.98 molal. This solution was bubbled with 30.2% (f-CO_2 = 0.302) CO_2-Ar to establish equilibrium. Buffer #3, p[H] 6.98. 36.5121 g (259.95 mmol) of $NaClO_4 \cdot H_2O$ and 0.8419 g (10.02 mmol) of $NaHCO_3$ were combined and dissolved with 100 mL distilled water in a volumetric flask to give a solution of composition 2.5998 M $NaClO_4$, 0.1002 M $NaHCO_3$, ρ = 1.1964 g/mL, and I = 3.10 molal. This solution was bubbled with 100% (f-CO_2 = 1.0) CO_2 to establish equilibrium. Buffer #4, p[H] 5.99. 36.8247 g (262.27 mmol). of $NaClO_4 \cdot H_2O$ and 0.0869 g (1.03 mmol) of $NaHCO_3$ were dissolved with 100 mL distilled water in a volumetric flask to give a solution of composition 2.6221 M $NaClO_4$, 0.0103 M $NaHCO_3$, ρ = 1.1886 g/mL, and I = 3.04 molal. This solution was bubbled with 100% (f-CO_2 = 1.0) CO_2 to establish equilibrium.

Ionic strength 2.5 m. p[H] was plotted against pH and linear regression gave the following pH correction for experiments at an ionic strength I_m = 2.5 mol/kg. p[H] = 1.00828(pH) + 0.520468, R^2 = 0.9999. Buffer #1, p[H] 8.65. 28.6538 g (204 mmol) of $NaClO_4 \cdot H_2O$, and 1.6800 g (20 mmol) of $NaHCO_3$ were dissolved with 100 mL distilled water in a volumetric flask to give a solution of composition 2.0403 M $NaClO_4$, 0.2 M $NaHCO_3$, ρ = 1.16 g/mL, and I = 2.52 molal. This solution was bubbled with 3% (f-CO_2 = 0.03) CO_2-Ar to establish equilibrium. Buffer #2, p[H] 7.71. 28.795 g (205 mmol) of $NaClO_4 \cdot H_2O$, and 1.6800 g (20 mmol) of $NaHCO_3$ were dissolved with 100 mL distilled water in a volumetric flask to give a solution of composition 2.0501 M $NaClO_4$, 0.2 M $NaHCO_3$, ρ = 1.16 g/mL, and I = 2.52 molal. This solution was bubbled with 30.2% (f-CO_2 = 0.302) CO_2-Ar to establish equilibrium. Buffer #3, p[H] 6.89. 30.1993 g (215 mmol) of $NaClO_4 \cdot H_2O$, and 0.8412 g (10 mmol) of $NaHCO_3$ were dissolved with 100 mL distilled water in a volumetric flask to give a solution of composition 2.150 M $NaClO_4$, 0.1001 M $NaHCO_3$, ρ = 1.17 g/mL, and I = 2.51 molal. This solution was bubbled with 100% (f-CO_2 = 1.0) CO_2-Ar to establish equilibrium. Buffer #4, p[H] 5.89. 31.3225 g (223 mmol) of $NaClO_4 \cdot H_2O$, and 0.084 g (1 mmol) of $NaHCO_3$ were dissolved with

100 mL distilled water in a volumetric flask to give a solution of composition 2.230 M $NaClO_4$, 0.010 M $NaHCO_3$, ρ = 1.17 g/mL, and I = 2.50 molal. This solution was bubbled with 100% (f-CO_2 = 1.0) CO_2-Ar to establish equilibrium.

Solution Preparations. ^{17}O - enriched solutions. Crystalline $UO_2(ClO_4)_2(H_2O)_6$ (0.577 g, 1.0 mmol) was dissolved in 2.5 mL of 20.4% $H_2{}^{17}O$ and 0.250 mL of 10.7 M ultra-pure $HClO_4$ to prepare a 20% ^{17}O-enriched solution of 0.4 *M* UO_2^{2+} ion in 1*M* $HClO_4$. This uranyl solution was electrolytically reduced to aquo U^{4+} using a conventional 3-electrode system at a potential of -0.22V (vs. SCE). The uranium solution was electrochemically re-oxidized to the UO_2^{2+} ion at about 1.10V (vs. SCE). This resulted in a UO_2^{2+} solution that was 10% enriched in ^{17}O. The oxidation states were confirmed using UV-VIS-NIR spectroscopy to identify the U(IV) peak at 648 nm (ε = 59 M^{-1} cm^{-1})[66] and the U(VI) peak at 414 nm (ε = 7.6 M^{-1} cm^{-1})[67] at each stage of the electrolysis. The $U^{17}O_2^{2+}$ was then precipitated as the hydroxide between 4.5 $\leq$ pH $\leq$ 7. The precipitate was isolated by centrifugation, and then washed 3 times with distilled, deionized H_2O. A solution of ^{17}O labeled carbonate was made by combining 2.32 mL of 43% $H_2{}^{17}O$, 2.4 mL D_2O, and 0.28 mL of 10.7 *M* supra-pure (carbonate-free) NaOH to make a 0.6 *M* NaOH solution. This solution was placed in a PARR pressure vessel and charged with 5 atmospheres of CO_2 with stirring. The solution was allowed to equilibrate for 48 h, to produce 5 mL of 0.6 *M* ^{17}O-enriched $NaHCO_3$. The ^{17}O-enriched uranyl hydroxide precipitate was dissolved in 4.25 mL of the freshly-prepared ^{17}O-enriched $NaHCO_3$. The resulting slurry was mixed on a vortex mixer for several minutes, then placed in an ultrasonic bath for 10 min until all the solid had dissolved, and a clear yellow solution resulted. $NaClO_4 \cdot H_2O$ (0.598 g, 7.1 mmol) was added to adjust the ionic strength to 3.3 mol/kg. 1*M* $HClO_4$ and solid Na_2CO_3 were used to adjust the pH and obtain samples in the pH range from 6.0 $\leq$ pH $\leq$ 9.7. Samples were sealed in 5mm NMR tubes, and solutions near a pH of 6 were stabilized by using CO_2 flushed NMR tubes. Samples flushed with CO_2 were not used in thermodynamic calculations.

Solution Preparations. ^{13}C - enriched solutions. Crystalline $UO_2(ClO_4)_2(H_2O)_6$ (1.739 g, 3.0 mmol) was dissolved in 2.0 mL D_2O. $Na_2{}^{13}CO_3$ (0.954 g, 8.9 mmol) and $NaClO_4(H_2O)$ (2.104 g, 25 mmol) were dissolved in 13 mL of D_2O in a 50 mL Oak Ridge centrifuge tube. The uranium solution was slowly added to this carbonate solution with stirring to make a solution which was 0.2 *M* in uranium, 0.6 *M* in sodium carbonate and 1.0 *M* in sodium perchlorate. 1*M* $HClO_4$ was used to adjust the pH of the solution to prepare 5 samples with pH values ranging from pH of 9.04 to 5.97. Samples were sealed in standard 5mm NMR tubes, those at lower pH were sealed in tubes flushed with CO_2 to maintain the pH. Another sample at I_m = 2.5 m was prepared similarly to make a solution which was 0.05 *M* in uranium, and 0.15 *M* in sodium carbonate, and 1.8 *M* in $NaClO_4$. 1*M* $HClO_4$ was used to adjust the pH of the solution to prepare 17 samples with pH values ranging from pH of 9.0 to 5.7. Samples were sealed in standard 5mm NMR tubes, those at lower pH were sealed in tubes flushed with CO_2 to maintain the pH.

Synthesis of $[C(NH_2)_3]_4[UO_2(CO_3)_3]$ (3). To a solution of 0.504 g (1.0 mmol) of $UO_2(NO_3)_2 \cdot 6\,H_2O$ in 0.5 mL of distilled water, a solution of 0.541 g (3.0 mmol) of guanidine carbonate in 9.5 mL of distilled water was added dropwise with stirring. The resulting 10 mL of solution was 0.1 *M* in uranium and 0.3 *M* in carbonate, and had a pH of 9.53. The solution was sealed in an argon purged 20 mL glass scintillation vial, wrapped in Parafilm, and stored at 0° C. After 24 hrs, large cubic crystals of a bright-yellow crystalline solid resulted. IR (KBr plates, Nujol, cm^{-1}) 3475 (vs, br), 1687 (s), 1526 (s), 1343 (s), 1143 (m), 1054 (m), 892(s), 866 (m), 811 (w), 687 (m), 530 (m). IR (KBr pellet, cm^{-1}) 1692(s) 1521(s, br), 1340 (s, br), 1139(m), 1046(m), 894(s), 860(m), 725(m), 684(w). Anal. Calcd. for $UO_{17}N_{12}C_7H_{24}$: C, 12.19; H, 3.50; N, 24.35. Found: C, 12.95; H, 3.22; N, 23.74.

Synthesis of $[C(NH_2)_3]_6[(UO_2)_3(CO_3)_6]$ (4). To a solution of 0.504 g (1.0 mmol) of $UO_2(NO_3)_2 \cdot 6\,H_2O$ in 0.5 mL of distilled water was added dropwise a solution of 0.541 g (3.0 mmol) of guanidine carbonate in 9.5 mL of distilled water with stirring. The resulting 10 mL of solution was 0.1 M in uranium and 0.3 M in carbonate. The pH of the uranyl carbonate solution was slowly lowered using 1M HCl, and a stream of CO_2 was passed over the solution to reach a final pH of 6.12. The solution was then sealed in a CO_2 purged 20 mL glass scintillation vial, wrapped in Parafilm, and stored at 0° C. After 24 hrs, thin needle-like plates of a bright-yellow crystalline solid resulted. IR (Nujol, KBr plates, cm^{-1}) 3352 (vs, br), 1672 (s), 1519 (s), 1464 (s), 1378 (s), 1339 (s), 1141 (m), 1047 (m), 886(s), 731 (s), 535 (m). IR (KBr pellet, cm^{-1}) 1668 (s), 1574 (m), 1528 (s), 1383 (s), 1333 (m), 1056 (w), 895(s), 835 (m), 728 (m), 713 (w). Anal. Calcd. for $U_3O_{24}N_{18}C_{12}H_{36}$: C, 9.42; H, 2.37; N, 16.47. Found: C, 10.21; H, 2.61; N, 19.00.

Synthesis of $[C(NH_2)_3]_6[(UO_2)_3(CO_3)_6] \cdot 6.5H_2O$ (5). A solution of 0.502 g (1.0 mmol) of $UO_2(NO_3)_2 \cdot 6\,H_2O$ in 5 mL of distilled water was added to 5 mL of aqueous guanidine carbonate (0.540g, 3.00 mmol) to yield a clear yellow solution. The pH of the resulting solution was adjusted to pH 7 using 0.1M $HClO_4$. Guanidine nitrate (0.732g, 6.00 mmol) was added and the solution was purged with CO_2. A fine white precipitate formed rapidly. The solution was stirred vigorously for several days, after which the solution was centrifuged and the supernatant was removed via pipette. The pH of the supernatant solution was measured to be 7.1. The solution was then blanketed with an atmosphere of CO_2 and cooled to 4°C. After two days, yellow cube-shaped crystals (believed to be $[C(NH_2)_3]_4[UO_2(CO_3)_4] \cdot nH_2O$) had formed. Slowly, yellow needle-shaped crystals of **5** began to form. After 30 days, several large needles had formed. IR (KBr, cm^{-1}) 3405(vs), 3377(sh), 3198(s), 1665(s), 1578(s,sh), 1530(s), 1371(s), 1149(w), 1047(m), 914(s), 892(s), 843(m), 728(m).

Raman Measurements. Raman vibrational spectra were obtained by excitation from an Ar^+ laser (Spectra Physics, Model 2025) using the 363.8 nm line. The laser power at the sample was ~10 mW. The scattered light was dispersed and analyzed on a SPEX Model 1403 Scanning Double Monochromator equipped with an 1800 groove/mm grating and a single-photon counting detector. The spectral slit width was maintained at 4 cm^{-1} resolution. Scan parameters were 1 cm^{-1} increments between points, integration for 2 sec at each point, and at least 60 scans averaged for the final spectrum. Spectra were recorded on ^{13}C-enriched samples in sealed 5mm NMR tubes.

EXAFS Studies. The EXAFS measurements were performed at the storage ring of the Stanford Synchrotron Radiation Laboratory (SSRL) on wiggler beamlines 4-3 and 4-1. Uranium L_{III} edge (~17.17 keV) spectra were recorded with Si(220) monochromator crystals (detuned 50% to reduce higher order harmonic content). All of the data were obtained from transmission experiments, in which argon gas ionization chamber detectors were employed. All spectra were collected simultaneously with uranium reference materials to establish the respective chemical shifts and to ensure photon energy calibrations. 8-10 scans of approximately one hour's duration were required to obtain good data on $[C(NH_2)_3]_6[(UO_2)_3(CO_3)_6]$ and the $[(UO_2)_3(CO_3)_6]^{6-}$-containing uranyl carbonate solution. Data analysis, including EXAFS curve fitting, was performed with the EXAFSPAK program suite, written by Graham N. George at SSRL. NMR studies of a duplicate sample of the uranyl carbonate solution used in the EXAFS experiments confirmed that the uranium was present as >97% $[(UO_2)_3(CO_3)_6]^{6-}$ both before and after data collection.

Crystallographic Studies. Crystal data, data collection, and processing parameters are given in Table III. Crystals of **5** suitable for an X-ray diffraction study were grown from aqueous

solution at 4 °C under an atmosphere of CO_2. Several needle-like crystals were mounted on glass fibers and checked for suitability for data collection. The first four crystals either diffracted too weakly, or showed evidence of crystal twinning. A crystal measuring 0.15 x 0.25 x 0.25 mm was obtained by cutting a section from a large needle. This crystal was affixed to the end of a glass fiber using silicone grease and transferred to the goniostat of a Siemens R3m/V Diffractometer where it was cooled to -44 °C for characterization and data collection. Unit cell parameters were determined from the least-squares refinement of 50 accurately-centered reflections. A systematic search of a limited hemisphere of reciprocal space located a set of diffraction maxima with triclinic symmetry and extinctions corresponding to one of the space groups P1 or P1bar. Subsequent solution and refinement of the structure revealed the centrosymmetric space group, P1bar, to be the correct choice. Two reflections were chosen as intensity standards and measured every 3600 s of X-ray exposure, and two orientation controls were measured every 250 reflections. Data were collected by omega scans.

Equivalent reflections were merged and systematically absent reflections were rejected. The intensities were corrected for Lorentz and polarization effects, and an analytical absorption correction was applied. The structure was easily solved by routine Patterson and Fourier methods. Attempts to refine the carbon atoms anisotropically were successful with the exception of C(6) in a terminal carbonate ligand, and C(51) in one guanidinium cation, which converged to non-positive definite thermal values. It was decided to leave the one guanidinium molecule and C(6) isotropic, while all other atoms were refined anisotropically. In the final cycles, hydrogen atoms were introduced in fixed, idealized positions, and were constrained to "ride" upon the appropriate carbon atoms. Final refinement using 5482 unique observed ($F > 3\sigma(F)$) reflections converged at R = 0.0546, R_w = 0.0615 (where $w = 1/[\sigma^2(F)^2 + 0.000625F^2]$) and GOF = 1.36. All calculations were performed using the SHELXTL PLUS suite of computer programs (Siemens Analytical X-ray Instr., Inc. 1991).

Acknowledgment. We wish to thank Professors K. N. Raymond (Berkeley), T. W. Newton (LANL), and W. Rees (Georgia Tech) for helpful discussions, and the Chemical Science and Technology Division (via Dr. A. P. Sattelberger) for ^{17}O-enriched water. This research was sponsored by the Office of Basic Energy Sciences, Division of Chemical Sciences, U.S. Department of Energy under contract W-7405-eng-36 with the University of California and by the Yucca Mountain Site Characterization Project Office as part of the Civilian Radioactive Waste Management Program managed by the U.S. Department of Energy, Nevada Operations Office. M. P. Neu is the recipient of a U. C. Presidents postdoctoral fellowship.

Supplementary Material Available: Complete summary of crystallographic data, fractional coordinates for all atoms, tables of bond lengths and angles, anisotropic thermal parameters for **5**, tables listing solution conditions for equilibrium constants and buffer compositions, and ORTEP drawings of **5** (46 pages). Ordering information is given on any current masthead page.

References

1. a) Lawrence Berkeley National Laboratory, Mail Stop 70A-1150, b) Los Alamos National Laboratory, Mail Stop G739, c) Glenn T. Seaborg Institute, d) Institute für Radiochemie.
2. Choppin, G. R.; Stout, B. E. *Sci. Tot. Environ.* **1989**, *83*, 203.
3. Choppin, G. R.; Allard, B. in *Handbook of the Chemistry and Physics of the Actinides*; Freeman, A. J., Keller, C., Eds.; Elsevier, Amsterdam, **1985**; Vol 3, Chapter 11.
4. Nash, K. L.; Cleveland, J. M.; Rees, T. F. *J. Environ. Radioactivity*, **1988**, *7* , 131.
5. Kim, J. I. in *Handbook of the Chemistry and Physics of the Actinides*; Freeman, A. J., Keller, C., Eds.; Elsevier, Amsterdam, **1986**; Vol 4, Chapter 8.
6. Hobart, D. E. in *Proceedings of the Robert A. Welch Foundation Conference on Chemical Research XXXIV: Fifty Years with Transuranium Elements*, Chapter XIII, Houston, TX, October 22-24, **1990**, 379, and references therein.

7. Grenthe, I.; Lemire, R. J.; Muller, A. B.; Nguyen-Trung, C.; Wanner, H.; *Chemical Thermodynamics of Uranium*; OEDC-NEA: Paris, **1991.**

8. Christ, C. L.; Clark, J. R.; Evans, H. T., Jr. *Science*, **1955**, *121*, 472.

9. Apelman, D. *Geol. Soc. Am. Bull.*, **1956**, 67, 1666.

10. Coda, A.; Della Giusta, A.; Tazzoli, V. *Acta. Cryst.* **1981**, *B37*, 1496.

11. Blake, C. A.; Coleman, C. F.; Brown, K. B.; Hill, D. G.; Lowrie, R. S.; Schmitt, J. M. *J. Am. Chem. Soc.*, **1956**, *78*, 5978.

12. Paramonova, V. I.; Nikol'skii, B. P.; Nikolaeva, N. M. *Russ. J. Inorg. Chem.*, **1962**, *7*, 528.

13. Sergeyeva, E. I.; Nikitin, A. A.; Khodakovsky, I. L.; Naumov, G. B. *Geochim. Int.*, **1972**, *11*, 900.

14. Almagro, V.; Garcia, F. S.; Sancho, *J. An. Quim.*, **1973**, *69*, 709.

15. Cinnéide, S. O.; Scanlan, J. P.; Hynes, M. J., *J. Inorg. Nucl. Chem.* **1975**, *37*, 1013.

16. Nikolaeva, N. M., *Izv. Sib. Otd. Akad. Nauk SSSR*, **1976**, *6*, 30.

17. Ciavatta, L.; Ferri, D.; Grimaldi, M.; Palombari, R.; Salvatore, F. *J. Inorg. Nucl. Chem.* **1979**, *41*, 1175.

18. Maya, L.; Begun, G. M. *J. Inorg. Nucl. Chem.* **1981**, *43*, 2827.

19. Ferri, G.; Grenthe, I.; Salvatore, F. *Acta Chem. Scand.* **1981**, *A35*, 165.

20. Maya, L. *Inorg. Chem.* **1982**, *21*, 2895.

21. Grenthe, I.; Ferri, D.; Salvatore, F.; Riccio, G. *J. Chem. Soc. Dalton Trans.* **1984**, 2439.

22. Grenthe, I.; Lagerman, B. *Acta Chem. Scand.* **1991**, *45*, 122.

23. Ullman, W. J.; Schreiner, F. *Radiochim. Acta.* **1988**, *43*, 37.

24. Ciavatta, L.; Ferri, D.; Grenthe, I.; Salvatore, F. *Inorg. Chem.* **1981**, *20*, 463.

25. Åberg, M.; Ferri, D.; Glaser, J.; Grenthe, I. *Inorg. Chem.* **1983**, *22*, 3981

26. B. E. Stout, G. R. Choppin, and J. C. Sullivan, in *Transuranium Elements, A Half Century*, L. R. Morss, and J. Fuger, Eds. American Chemical Society, Washington D.C.,**1992**, 225.

27. Brücher, E.; Glaser, J.; Toth, I. *Inorg. Chem.*, **1991**, *30*, 2239.

28. Strom, E. T.; Woessner, D. E.; Smith, W. B. *J. Am. Chem. Soc.*, **1981**, *103* , 1255.

29. Graziani, R.; Bombieri, G.; Forsellini, E. *J. Chem. Soc., Dalton Trans.* **1972**, *19*, 2059.

30. Mereiter, K. *Acta Crystallogr.* **1988**, *C44*, 1175.

31. Simakin, G. A. *Radiokhimiya* **1977**, *19* , 424.

32. Maya, L. *Inorg. Chem.* **1984**, *23*, 3926.

33. Marquart, R.; Hoffmann, G.; Weigel, F. *J. Less-Common Met.*, **1983**, *91*, 119.

34. Madic, C.; Hobart, D. E.; Begun, G. M. *Inorg. Chem.* **1983**, *22*, 1494.

35. Basile, L. J.; Ferraro, J. R.; Mitchell, M. L.; Sullivan, J. C. *Appl. Spectroscopy* **1978**, *32*, 535.

36. Nguyen-Trung, C.; Begun, G. M.; Palmer, D. A. *Inorg. Chem.* **1992**, *31*, 5280.

37. Grenthe, I.; Riglet, C.; Vitorge, P. *Inorg. Chem.*, **1986**, *25*, 1679.

38. Ferri, D.; Glaser, J.; Grenthe, I. *Inorg. Chim. Acta*, **1988**, *148*, 133.

39. Figgis, B. N.; Kidd, R. G.; Nyholm, R. S. *Proc. Royal Soc. A.*, **1962**, *A269*, 469.

40. Boykin, D. W. *^{17}O NMR Spectroscopy in Organic Chemistry*, CRC Press, Boca Raton, **1991**.

41. Klemperer, W. G. *Angew Chem. Int. Ed., Engl.* **1978**, *17*, 246.

42. Jung, W-S.; Ikeda, Y.; Tomiyasu, H.; Fukutomi, H. *Bull. Chem. Soc. Japan*, **1984**, *57*, 2317.

43. Jung, W-S.; Tomiyasu, H.; Fukutomi, H. *Bull. Chem. Soc. Jpn*, **1985**, *58*, 938.

44. Jolivet, J. P.; Taravel, T. B.; Lorenzelli, V. *J. Molecular Structure*, **1980**, *60*, 93.

45. McGlynn, S. P.; Smith, J. K.; Neely, W. C. *J. Chem. Phys.* **1961**, *35*, 105.

46. Jones, L. H. *Spectrochimica Acta*, **1958**, *10*, 395.

47. Jones, L. H. *Spectrochimica Acta*, **1959**, *11*, 409.

48. Hoekstra, H. R. *Inorg. Chem.* **1963**, *2*, 492.

49. Bullock, J. I. *J. Chem. Soc. A.* **1969**, 781.

50. Mustre de Leon, J.; Rehr, J. J.; Zabinsky, S. I.; Albers, R. C. *Phys. Rev. B* **1991**, *44*, 4146.

51. Rehr, J. J.; Mustre de Leon, J.; Zabinsky, S. I.; Albers, R. C. *J. Am. Chem. Soc.* **1991**, *113*, 5135.

52. Teo, B. K. *J. Am. Chem. Soc.* **1981**, *103*, 3990.

53. Teo, B. K. *EXAFS: Basic Principles and Data Analysis;* Springer-Verlag: Berlin, 1986.

54. Garcia, J.; Delrio, M. S.; Buratini, E.; Benfatto, M. *Physica B* **1989**, *158*, 409.

55. Vedrinskii, R. V.; Bugaev, L. A.; Levin, I. G. *Physica B* **1989**, *158*, 421.

56. Bucher, J. J.; Edelstein, N. M.; Kaltsoyannis, N.; Lukens, W. W.; Shuh, D. K. unpublished results.

57. Anderson, A.; Chieh, C.; Irish, D. E.; Tong, J. P. K. *Can. J. Chem.* **1980**, *58*, 1651.

58 Mikhailov, Y. N.; Lobanova, G. M.; Shchelokov, R. N. *Russian J. Inorg. Chem.*, **1981**, *26*, 386.

59. Beirakhov, A. G.; Orlova, I. M.; Ashurov, Z. R.; Lobanova, G. M.; Mikhailov, Y.N.; Schelokov, R.N., *Russian J. Inorg. Chem.* **1991**, *36*, 369.

60. Westcott, C. C. *pH Measurements*, Academic Press, NY, **1978**.

61. Linder, P. W.; Torrington, R. G.; Williams, D. R. *Analysis Using Glass Electrodes*, Open University Press, Milton Keynes, **1984**.

62. Martell, A. E.; Motekaitis, R. J. *Determination and Use of Stability Constants*; VCH Publishers: New York, **1988**.

63. Baes, C. F.; Mesmer, R. E. *The Hydrolysis of Cations*, J. Wiley and Sons, N. Y. **1976**.

64. Robinson, R. A.; Stokes, R. H. *Electrolyte Solutions*, Butterworths Scientific. Publications, London, **1955**. pp 28.

65. Hobart, D. E.; Samhoun, K.; Peterson, J. R. *Radiochim. Acta.* **1982**, *31*, 139.

66. Kraus, K. A.; Nelson, F. *J. Amer. Chem. Soc.* **1950**, *72*, 3901.

67. Sjoblom, R.; Hindman, J. C. *J. Amer. Chem. Soc.* **1951**, *73*, 1744.

Table I. Structural Parameters from EXAFS Curve Fitting.

Shell	Coordination Number	r(Å)	Debye-Waller factor (Å)^2
Solid $[C(NH_2)_3]_6[(UO_2)_3(CO_3)_6]$			
U-O (uranyl)	2	1.79	0.0033
U-O (carbonate)	6	2.45	0.0080
U···C	3	2.90	0.0033
U···O (uranyl)[a]	-	3.60[b]	-
U···O (carbonate)	3	4.16	0.0064
U···U	2	4.91	0.0081
Solution $[(UO_2)_3(CO_3)_6]^{6-}$			
U-O (uranyl)	2	1.79	0.0026
U-O (carbonate)	6	2.46	0.0075
U···C	3	2.90	0.0039
U···O (uranyl)[a]	-	3.61[b]	-
U···O (carbonate)	3	4.17	0.0056
U···U	2	4.92	0.0087
Solid $K_4[UO_2(CO_3)_4]$			
U-O (uranyl)	2	1.79	0.0024
U-O (carbonate)	6	2.42	0.0059
U···C	3	2.89	0.0030
U···O (uranyl)[a]	-	3.59[b]	-
U···K	6	3.84	0 .0056
U···O (carbonate)	3	4.12	0.0046

[a] Multiple scattering peak. [b] Effective r

Table II. Average Uranium-Carbonate Distances (Å) from the X-ray Crystal Structures of $Na_2Ca[UO_2(CO_3)_3].xH_2O$ (x≈5.6) and $K_4[UO_2(CO_3)_3]$.

	$Na_2Ca[UO_2(CO_3)_3].xH_2O$ (X≈5.6)[a]	$K_4[UO_2(CO_3)_3]$[b]
U-O (uranyl)	1.80	1.80
U-O (carbonate)	2.44	2.43
U-C[c]	2.85	2.88
U-O[c] (carbonate)	4.14	4.12

[a] Data from reference 10 [b] Data from reference 57

[c] Distances calculated using an average of the reported carbonate C-O bond lengths and angles.

Table III. Summary of Crystallographic Data for $[C(NH_2)_3]_6[(UO_2)_3(CO_3)_6]\cdot 6.5H_2O$ (**5**)

Empirical Formula		$C_{12}\ H_{49}\ N_{18}\ O_{30.5}\ U_3$
Color; Habit		Yellow needle
Crystal dimen., mm		0.2 x 0.3 x 0.3
Space Group		P-1(#2)
Cell Dimen.	a, Å	6.941(2)
	b, Å	14.488(2)
	c, Å	22.374(2)
	α, deg	95.63(2)
	β, deg	98.47(2)
	γ, deg	101.88(2)
Volume, $Å^3$		2158.5
Z (molecules/cell)		2
Formula weight		1647.7
D_{calc}, g cm^{-3}		2.536
Absorption Coefficient, mm^{-1}		11.343
λ (Mo Kα)		0.71073
Temperature, °C		-44
Measured reflections		11695
Unique intensities		9784
Observed reflections		5482 ($F > 3\sigma(F)$)
R(F)[a]		0.0547
$R_w(F)$[b]		0.0616
Goodness-of-Fit		1.37

[a] $R(F) = \Sigma \left| |F_o| - |F_c| \right| / S |F_o|$. [b] $R_w(F) = [\Sigma w(|F_o| - |F_c|)^2 / \Sigma w|F_o|^2]^{1/2}$; $w = 1/\sigma^2(|F_o|)$.

Table IV. Selected Fractional Coordinates and Isotropic Thermal Parameters for the Uranyl Anion in $[C(NH_2)_3]_6[(UO_2)_3(CO_3)_6]\cdot 6.5H_2O$ (5)

	$10^4\,x$	$10^4\,y$	$10^4\,z$	$10\,B(iso)$
U(1)	2944(1)	7179(1)	592(1)	16(1)
U(2)	4520(1)	7183(1)	830(1)	16(1)
U(3)	1937(1)	4123(1)	453(1)	15(1)
O(101)	373(20)	7135(9)	6609(6)	27(5)
O(102)	5507(20)	7214(8)	6563(6)	25(5)
O(201)	7068(20)	7181(10)	8832(7)	32(5)
O(202)	1956(20)	7188(9)	8835(6)	25(5)
O(301)	4406(19)	3985(9)	7414(6)	26(5)
O(302)	-501(20)	4287(9)	7493(6)	31(5)
C(1)	1930(29)	5114(14)	6383(8)	22(7)
O(1)	2494(22)	5567(8)	6957(6)	29(5)
O(2)	1932(20)	5611(8)	5967(5)	22(5)
O(3)	1387(20)	4214(8)	6355(6)	24(5)
C(2)	3392(27)	5132(12)	8667(8)	18(6)
O(4)	3494(20)	5583(8)	8181(5)	24(5)
O(5)	4021(18)	5620(8)	9185(6)	20(4)
O(6)	2635(20)	4242(8)	8576(5)	24(5)
C(3)	4274(30)	8243(13)	7798(10)	29(7)
O(7)	3895(22)	7296(8)	7726(6)	26(5)
O(8)	4884(21)	8653(9)	8348(6)	28(5)
O(9)	4014(20)	8637(9)	7335(6)	27(5)
C(4)	2773(30)	8217(12)	5571(8)	22(7)
O(11)	2772(31)	8673(10)	5111(7)	60(8)
O(12)	3166(22)	8632(9)	6137(6)	34(5)
O(13)	2483(19)	7290(8)	5518(6)	24(5)
C(5)	5545(29)	8173(14)	10027(9)	25(7)
O(21)	6084(21)	8638(8)	10554(6)	29(5)
O(22)	5485(20)	8610(8)	9553(5)	24(5)
O(23)	5142(20)	7278(8)	9919(5)	22(4)
C(6)	719(30)	2081(14)	7340(9)	27(5)
O(31)	360(22)	1215(8)	7282(6)	33(5)

Table IV (cont.)

O(32)	1182(19)	2633(9)	7858(6)	25(5)
O(33)	610(20)	2572(9)	6855(6)	25(5)

Table V. Selected Bond Distances (Å) and Bond Angles (°) for the Uranyl Anion in $[C(NH_2)_3]_6[(UO_2)_3(CO_3)_6]\cdot 6.5H_2O$ (5)

U(1)	U(2)	4.965(1)	U(1)	U(3)	4.959(1)	U(2)	O(7)	2.471(12)
U(1)	O(101)	1.779(14)	U(1)	O(102)	1.780(14)	U(2)	O(23)	2.397(12)
U(1)	O(1)	2.523(12)	U(1)	O(9)	2.466(12)	U(3)	O(302)	1.771(15)
U(1)	O(2)	2.457(10)	U(1)	O(12)	2.414(14)	U(3)	O(1)	2.451(12)
U(1)	O(7)	2.507(12)	U(2)	U(3)	4.978(1)	U(3)	O(6)	2.470(12)
U(1)	O(13)	2.402(12)	U(2)	O(202)	1.783(14)	U(3)	O(32)	2.412(13)
U(2)	O(201)	1.769(14)	U(2)	O(4)	2.518(11)	U(3)	O(33)	2.426(11)
U(2)	O(5)	2.447(12)	U(2)	O(8)	2.464(13)	U(3)	O(3)	2.451(13)
U(2)	O(22)	2.407(11)	U(3)	O(4)	2.482(10)	U(3)	O(301)	1.779(14)

O(101)	U(1)	O(102)	179.1(6)	O(201)	U(2)	O(202)	179.4(5)
O(301)	U(3)	O(302)	178.8(6)	U(3)	O(4)	C(2)	93.7(9)
O(1)	U(1)	O(2)	52.4(4)	U(1)	O(7)	U(2)	171.8(5)
O(1)	U(1)	O(7)	67.7(4)	O(1)	U(3)	O(3)	53.1(4)
(1)	O(1)	C(1)	92.1(11)	O(3)	U(3)	O(6)	173.1(4)
(2)	O(4)	U(3)	169.1(6)	O(4)	U(3)	O(6)	53.3(4)
O(2)	U(1)	O(9)	172.4(4)	O(1)	U(3)	O(32)	174.8(4)
O(7)	U(1)	O(9)	52.5(4)	O(4)	U(2)	O(5)	53.0(4)
O(1)	U(1)	O(12)	173.7(4)	U(2)	O(8)	C(3)	96.2(11)
O(1)	U(3)	O(4)	67.0(4)	O(11)	C(4)	O(12)	123.4(16)
O(9)	U(1)	O(12)	66.0(4)	O(11)	C(4)	O(13)	122.6(16)
O(2)	U(1)	O(13)	67.5(4)	U(2)	O(22)	C(5)	95.1(10)
O(7)	U(1)	O(13)	170.5(4)	U(3)	O(32)	C(6)	97.3(11)
O(12)	U(1)	O(13)	54.3(4)	U(3)	O(33)	C(6)	95.0(9)
O(22)	C(5)	O(23)	115.3(15)	O(1)	C(1)	O(3)	113.6(16)
O(6)	U(3)	O(32)	64.8(4)	O(2)	C(1)	O(3)	129.2(15)
O(4)	U(2)	O(7)	66.9(4)	U(1)	O(1)	U(3)	171.2(6)
U(1)	O(7)	C(3)	92.7(11)	U(3)	O(1)	C(1)	95.6(10)
U(1)	O(7)	C(3)	149.0(12)	U(1)	O(2)	C(1)	98.3(10)
O(5)	U(2)	O(8)	173.1(4)	U(3)	O(3)	C(1)	97.6(10)
O(7)	U(2)	O(8)	53.3(4)	O(3)	U(3)	O(33)	67.7(4)
O(4)	U(2)	O(22)	173.2(4)	O(4)	U(3)	O(33)	171.7(4)

Table V (cont.)

O(12)	C(4)	O(13)	113.9(16)	O(32)	U(3)	O(33)	54.4(4)
O(8)	U(2)	O(22)	66.6(4)	O(1)	C(1)	O(2)	117.1(16)
U(2)	O(23)	C(5)	96.3(11)	U(2)	O(4)	C(2)	91.9(9)
O(5)	U(2)	O(23)	67.0(4)	U(2)	O(5)	C(2)	96.8(11)
O(7)	U(2)	O(23)	173.0(4)	U(3)	O(6)	C(2)	95.7(10)
O(22)	U(2)	O(23)	53.2(4)	U(1)	O(9)	C(3)	97.1(11)

Table VI. Comparison of X-ray and EXAFS Metrical Parameters

	X-ray		EXAFS	
	Solid	Solution	Solid	Solution
$UO_2(CO_3)_3^{4-}$				
U=O	1.80 (a)		1.79 (b)	
U-O (CO_3^{2-})	2.43		2.42	
U--C	2.88		2.89	
O=U=O	3.60		3.59	
U---O (CO_3^{2-})	4.12		4.12	
U---K	3.83	--	3.84	--
$(UO_2)_3(CO_3)_6^{6-}$				
U=O	1.77 (b)		1.79 (b)	1.79 (b)
U-O (CO_3^{2-})	2.46		2.45	2.46
U--C	2.88		2.90	2.90
O=U=O	3.54		3.60	3.61
U---O (CO_3^{2-})	4.14		4.16	4.17
U---U	4.97	4.95 (c)	4.91	4.92

(a) Ref 29

(b) This work.

(c) Ref 25

Table VII. Thermodynamic Binding Constants for the Uranyl Carbonate System used in this study[a]

			$I_m = 0$	2.5	3.0
Ligand Data					
$CO_3^{2-} + H^+ \rightleftharpoons HCO_3^-$	log K =		10.33	9.68	9.71
$CO_3^{2-} + 2H^+ \rightleftharpoons CO_2\,(aq) + H_2O$	log K =		16.68	15.82	15.90
$HCO_3^- + H^+ \rightleftharpoons CO_2\,(g) + H_2O$	log K =		7.82	7.65	7.70
Metal Complex Data					
$UO_2^{2+} + CO_3^{2-} \rightleftharpoons UO_2(CO_3)\,(aq)$	log β_{11} =		9.63	8.87	9.05
$UO_2^{2+} + 2\,CO_3^{2-} \rightleftharpoons UO_2(CO_3)_2^{2-}$	log β_{12} =		16.94	15.78	15.88
$UO_2^{2+} + 3\,CO_3^{2-} \rightleftharpoons UO_2(CO_3)_3^{4-}$	log β_{13} =		21.63	22.18	22.29
$3\,UO_2^{2+} + 6\,CO_3^{2-} \rightleftharpoons (UO_2)_3(CO_3)_6^{6-}$	log β_{36} =		54.00	55.32	55.59
Metal Hydrolysis Data					
$UO_2^{2+} + H_2O \rightleftharpoons UO_2(OH) + H^+$	log β_{1-1} =		-5.20	-4.71	-4.54
$2\,UO_2^{2+} + H_2O \rightleftharpoons (UO_2)_2(OH)^{3+}$	log β_{2-1} =		-2.70	-2.26	-2.25
$UO_2^{2+} + 2\,H_2O \rightleftharpoons UO_2(OH)_2 + 2H^+$	log β_{1-2} =		-10.30	-10.40	-10.34
$2\,UO_2^{2+} + 2\,H_2O \rightleftharpoons (UO_2)_2(OH)_2^{2+} + 2H^+$	log β_{2-2} =		-5.62	-6.05	-6.05
$3\,UO_2^{2+} + 4\,H_2O \rightleftharpoons (UO_2)_3(OH)_4^{2+} + 4H^+$	log β_{3-4} =		-11.90	-13.25	-13.36
$3\,UO_2^{2+} + 7\,H_2O \rightleftharpoons (UO_2)_3(OH)_7^- + 7H^+$	log β_{3-7} =		-31.00	-32.46	-32.60
$3\,UO_2^{2+} + 5\,H_2O \rightleftharpoons (UO_2)_3(OH)_5^+ + 5H^+$	log β_{3-5} =		-15.55	-16.74	-16.74
$4\,UO_2^{2+} + 7\,H_2O \rightleftharpoons (UO_2)_4(OH)_7^+ + 7H^+$	log β_{4-7} =		-21.90	-23.17	-23.10

[a] Values at $I_m = 0$ taken from ref 7 and corrected using SIT

Figure Captions

Figure 1. (a). ^{13}C NMR spectra (62.9 MHz) of a 0.2M uranyl carbonate solution at 23 °C as a function of pH. **(b).** ^{13}C NMR spectra of the same 0.2M uranyl carbonate solution recorded at 0 °C. Carbon resonances corresponding to $UO_2(CO_3)_3^{4-}$ and $(UO_2)_3(CO_3)_6^{6-}$ are indicated. Ionic strength = 4.0 m.

Figure 2. ^{13}C NMR spectra (62.9 MHz) of a 0.05M uranyl carbonate solution at 2.5 m ionic strength as a function of pH recorded at 0 °C.

Figure 3. ^{17}O NMR spectrum (33.9 MHz) of fully ^{17}O-enriched $UO_2(CO_3)_3^{4-}$ at pH 9.7 and 0 °C.

Figure 4. Expanded uranyl region of the ^{17}O NMR spectrum (33.9 MHz) of a 0.2M $UO_2(CO_3)_3^{4-}$ solution as a function of pH at 0 °C.

Figure 5. The EXAFS spectrum and its Fourier transform (uncorrected for phase shift) of solid $[C(NH_2)_3]_6[UO_2(CO_3)_2]_3$. The solid line is the experimental data and the dashed line a best fit.

Figure 6. The EXAFS spectrum and its Fourier transform (uncorrected for phase shift) of $[(UO_2)_3(CO_3)_6]^{6-}$ in solution. The solid line is the experimental data and the dashed line a best fit.

Figure 7. The EXAFS spectrum and its Fourier transform (uncorrected for phase shift) of solid $K_4[UO_2(CO_3)_3]$. The solid line is the experimental data and the dashed line a best fit.

Figure 8. An ORTEP of the $(UO_2)_3(CO_3)_6^{6-}$ anion giving the atom number scheme used in the Tables.

Figure 9. A ball and stick drawing looking down the crystallographic b axis, and illustrating the packing of ions in $[C(NH_2)_3]_6[(UO_2)_3(CO_3)_6]\cdot 6.5H_2O$.

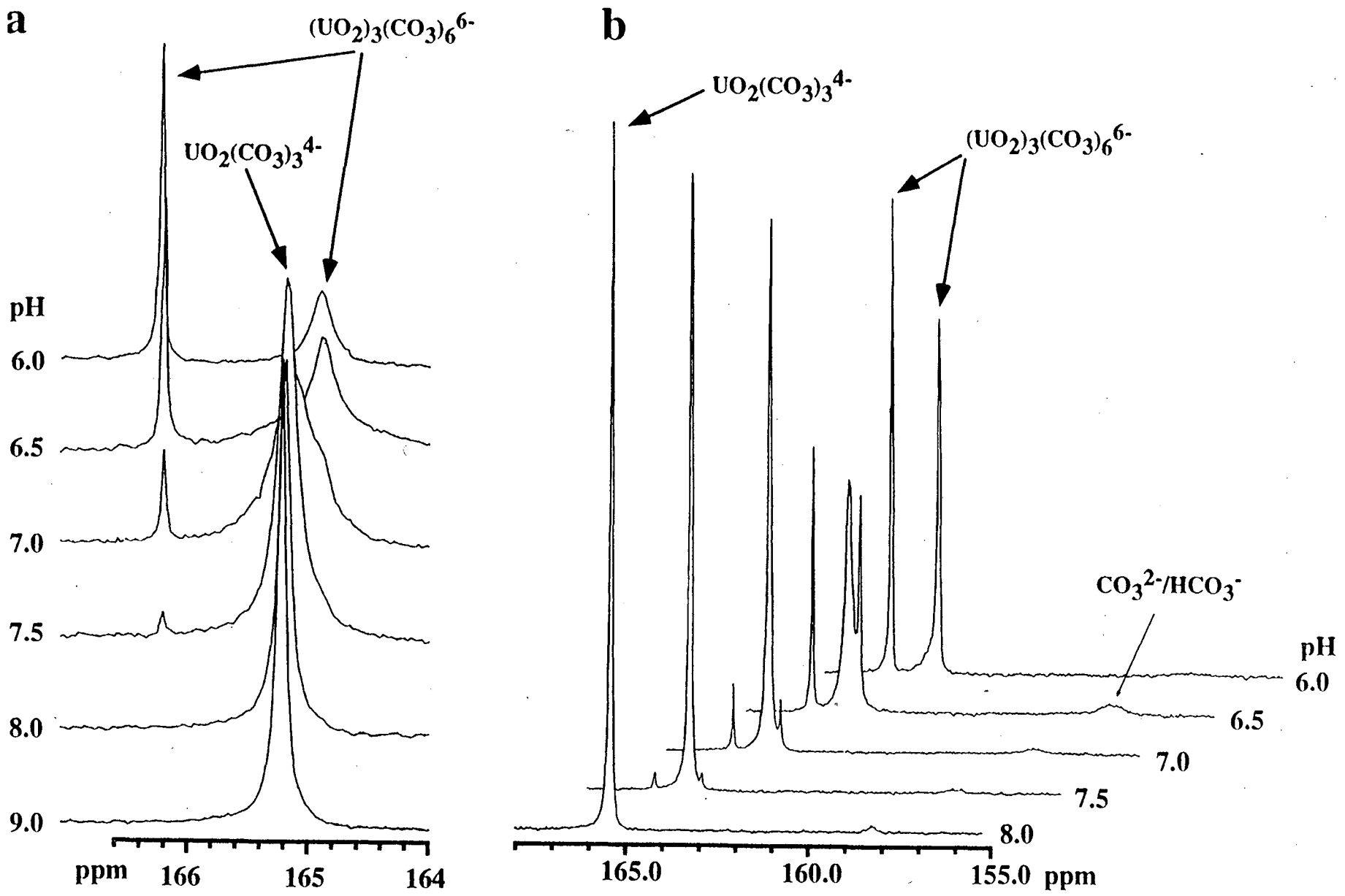
a
$(UO_2)_3(CO_3)_6^{6-}$
$UO_2(CO_3)_3^{4-}$
pH
6.0
6.5
7.0
7.5
8.0
9.0
ppm
166
165
164
b
$UO_2(CO_3)_3^{4-}$
$(UO_2)_3(CO_3)_6^{6-}$
CO_3^{2-}/HCO_3^-
pH
6.0
6.5
7.0
7.5
8.0
165.0
160.0
155.0 ppm

Figure 1

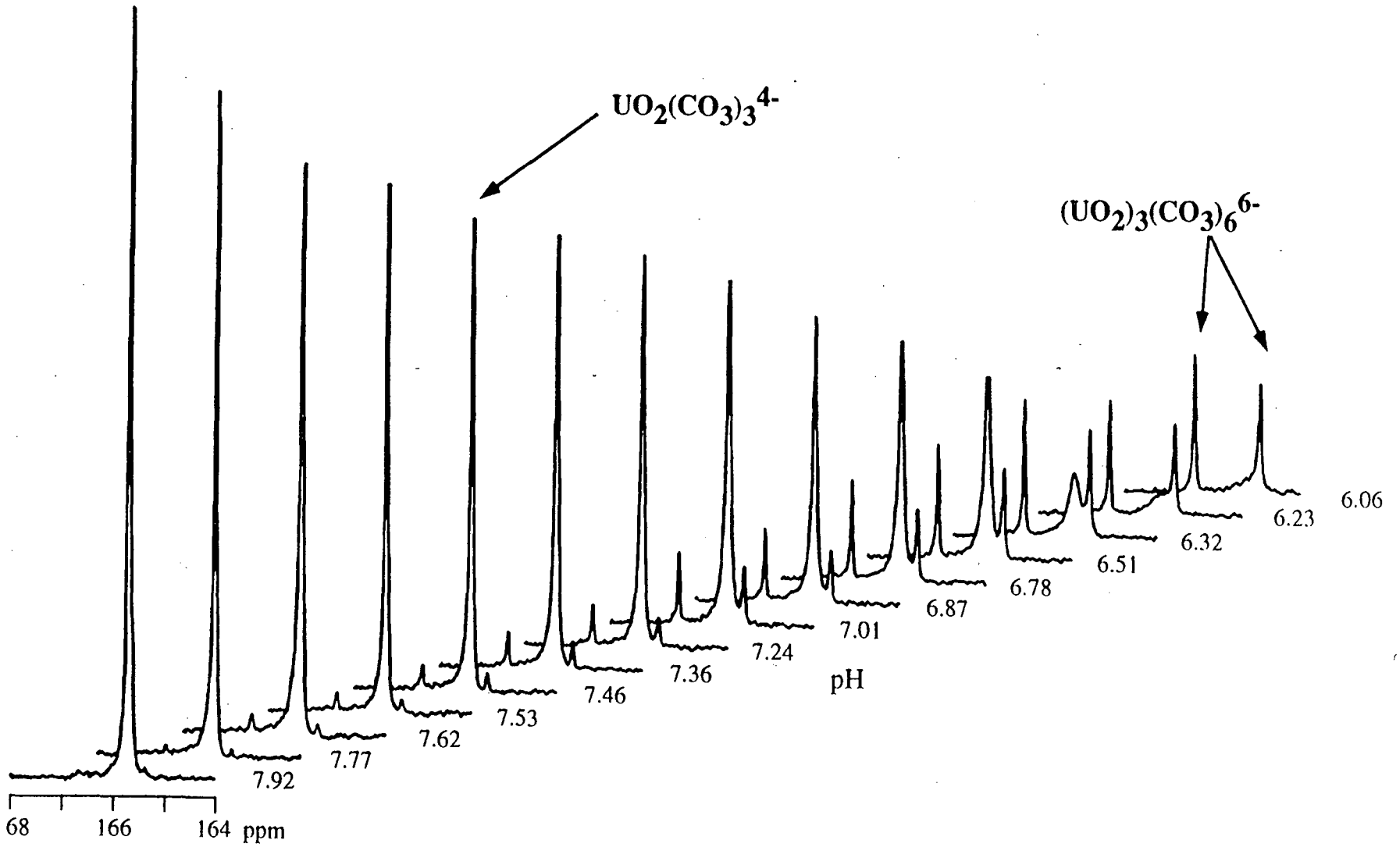
$UO_2(CO_3)_3^{4-}$
$(UO_2)_3(CO_3)_6^{6-}$
6.06
6.23
6.32
6.51
6.78
6.87
7.01
7.24
7.36
7.46
7.53
7.62
7.77
7.92
pH
68
166
164 ppm

Figure 2

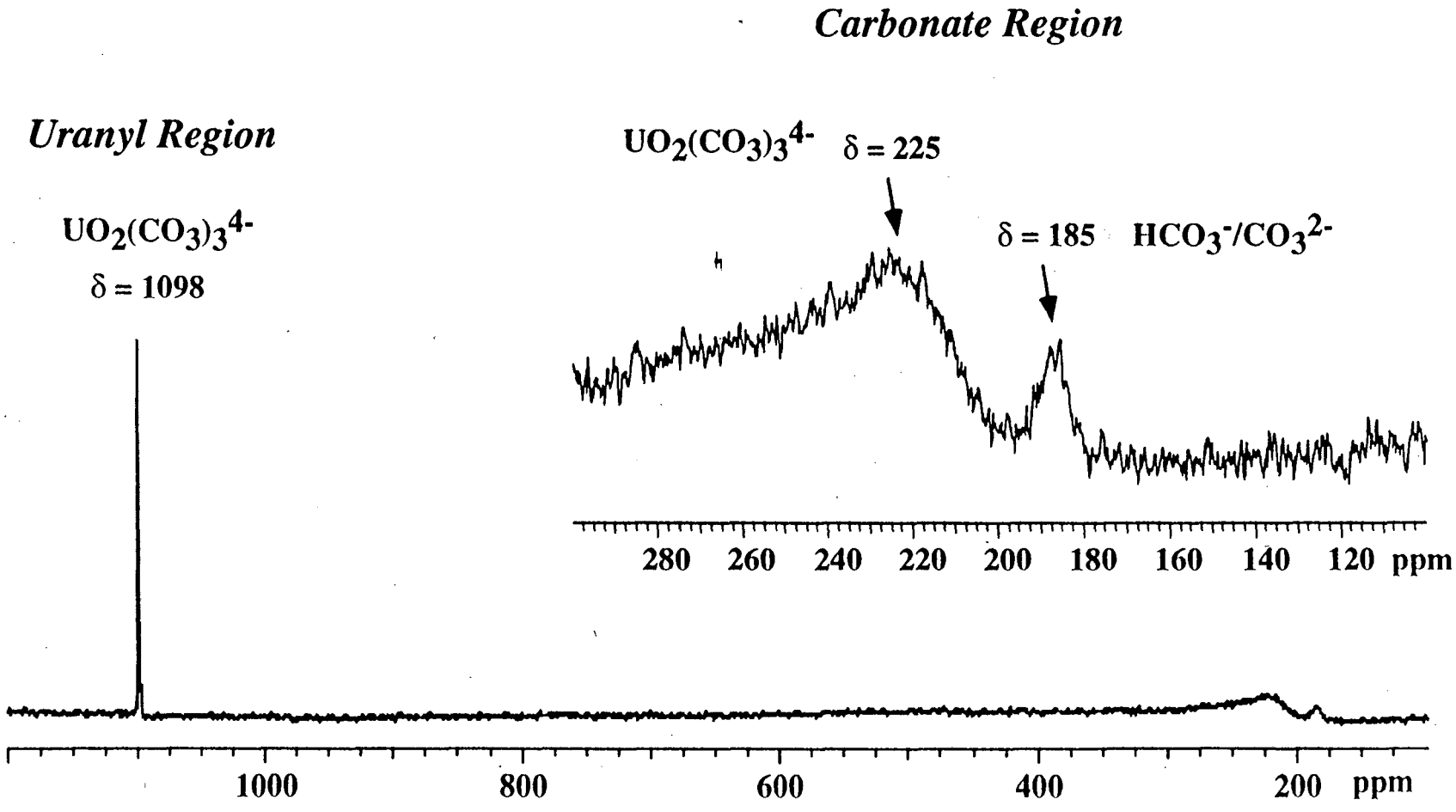
Carbonate Region
Uranyl Region
UO2(CO3)3 4-
δ = 225
δ = 185
HCO3-/CO3 2-
UO2(CO3)3 4-
δ = 1098
280
260
240
220
200
180
160
140
120
ppm
1000
800
600
400
200
ppm

Figure 3

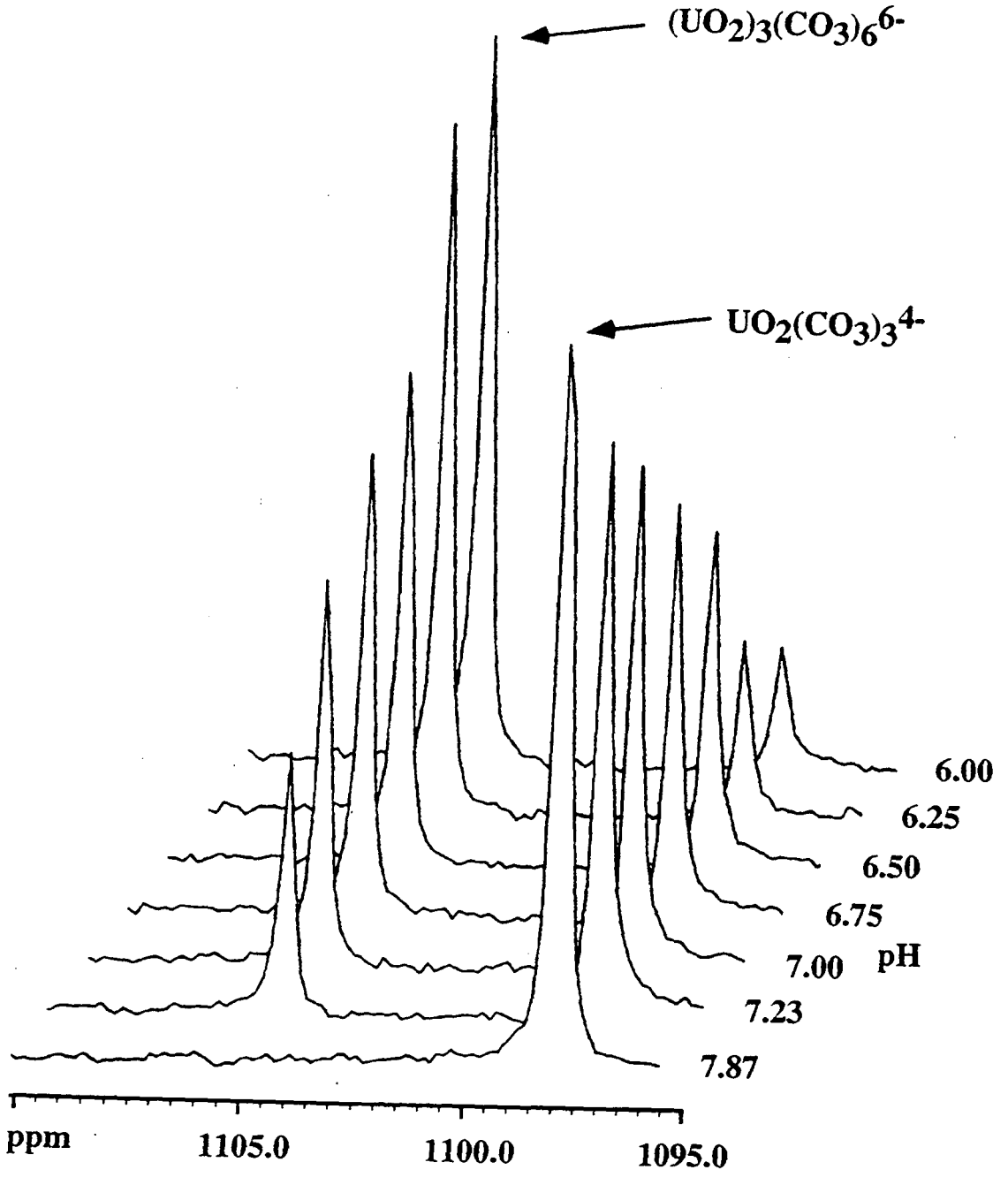
$(UO_2)_3(CO_3)_6^{6-}$
$UO_2(CO_3)_3^{4-}$
6.00
6.25
6.50
6.75
7.00
pH
7.23
7.87
ppm
1105.0
1100.0
1095.0

Figure 4

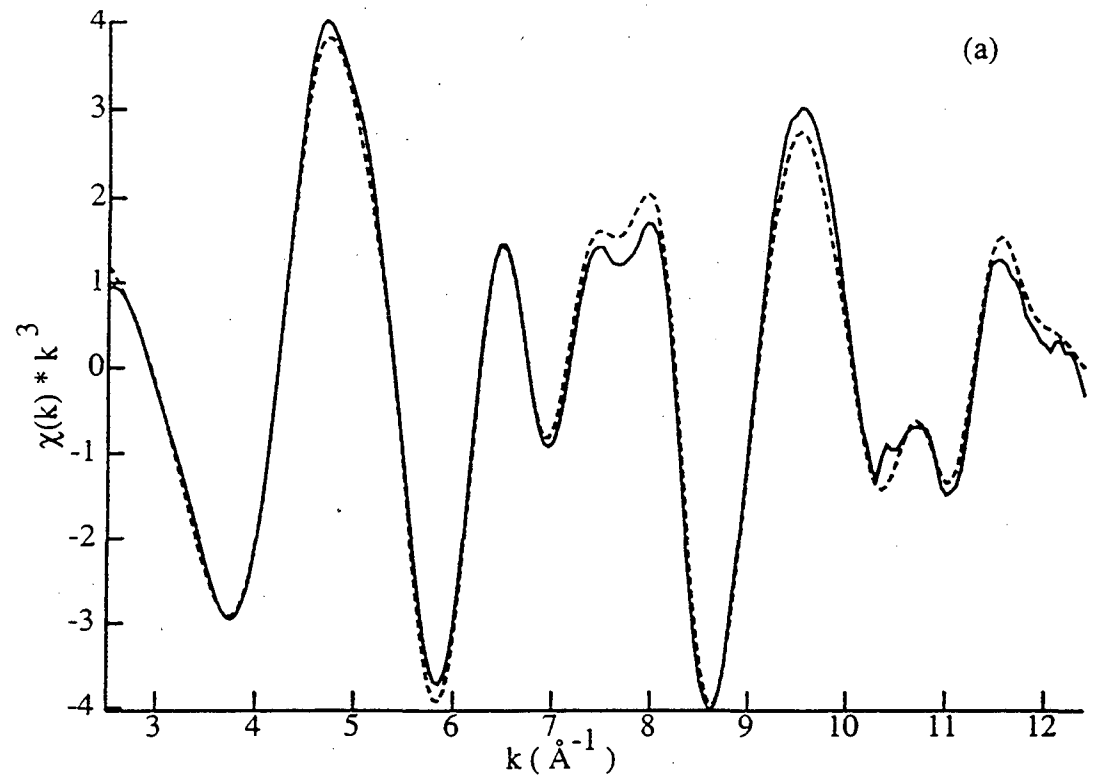

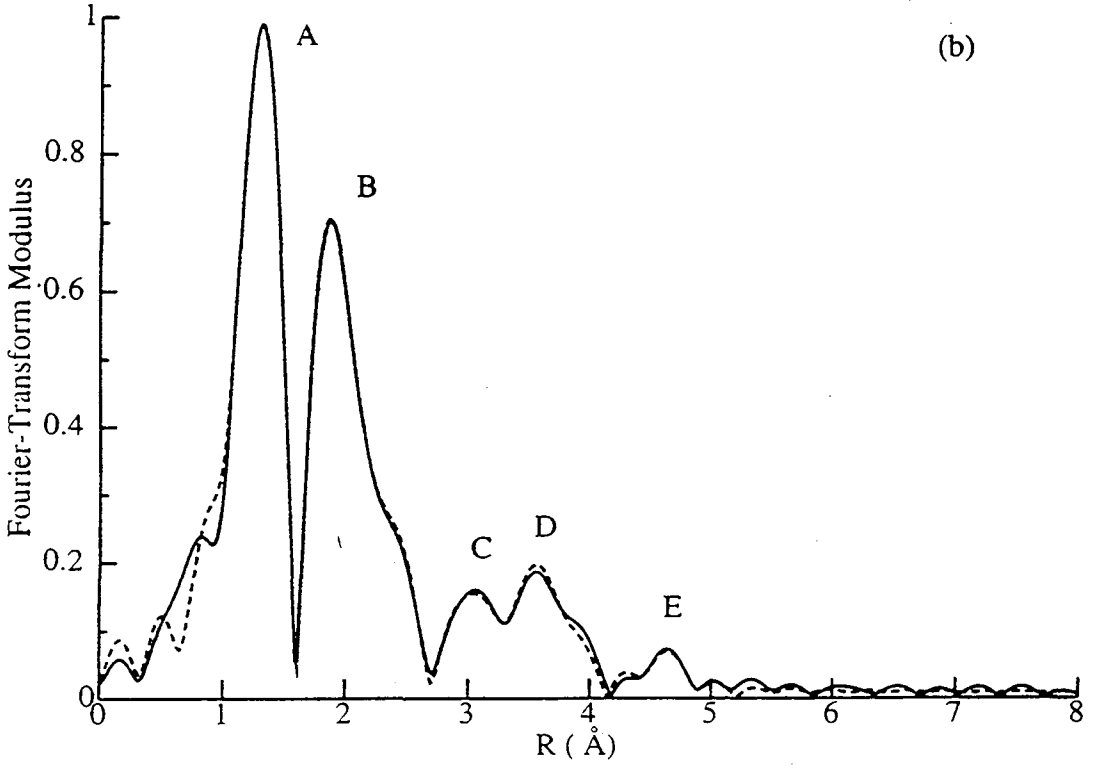

Figure 5

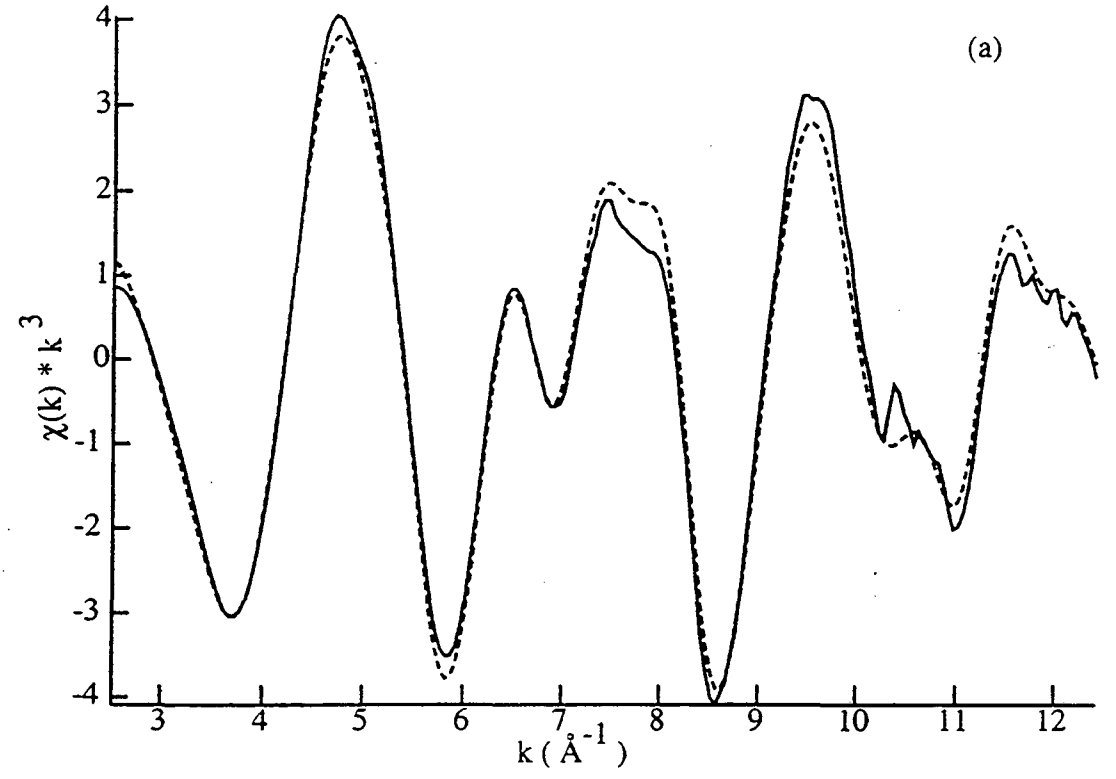

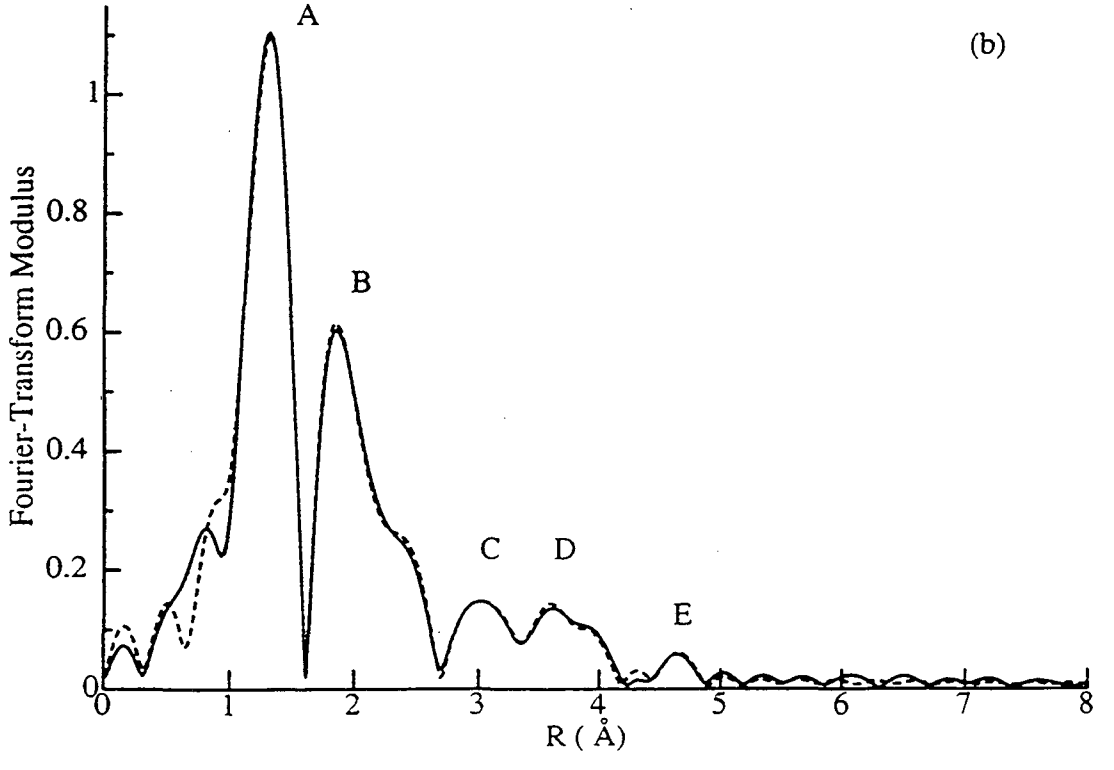

Figure 6

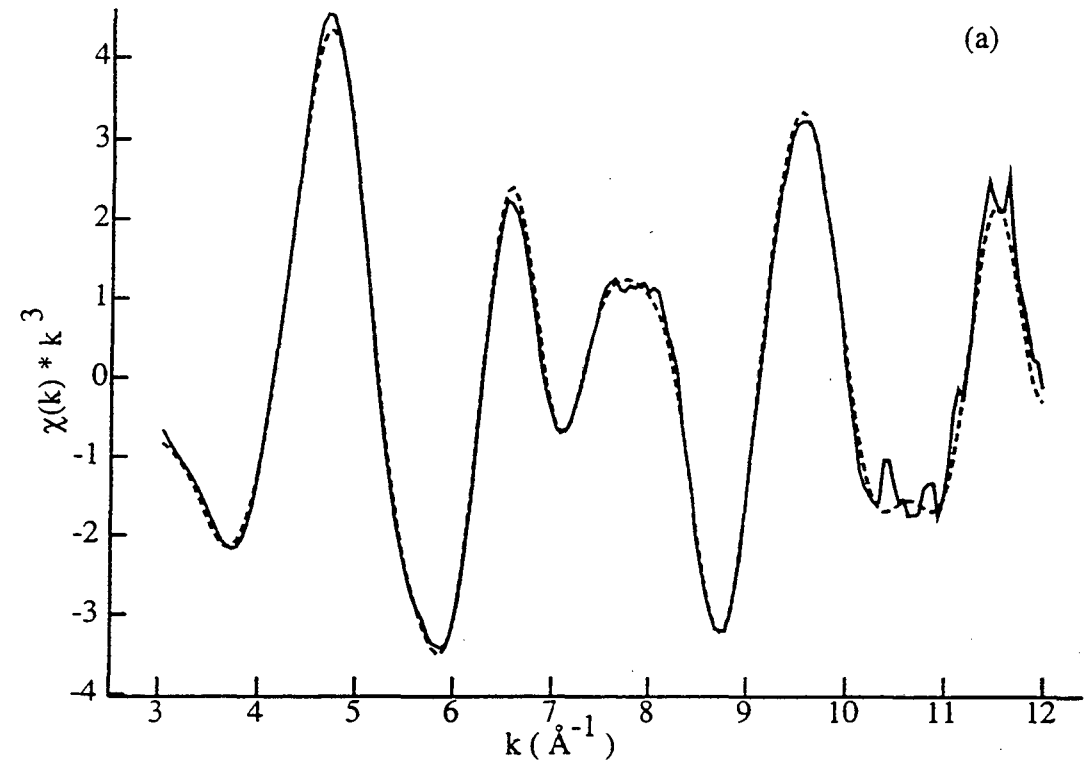

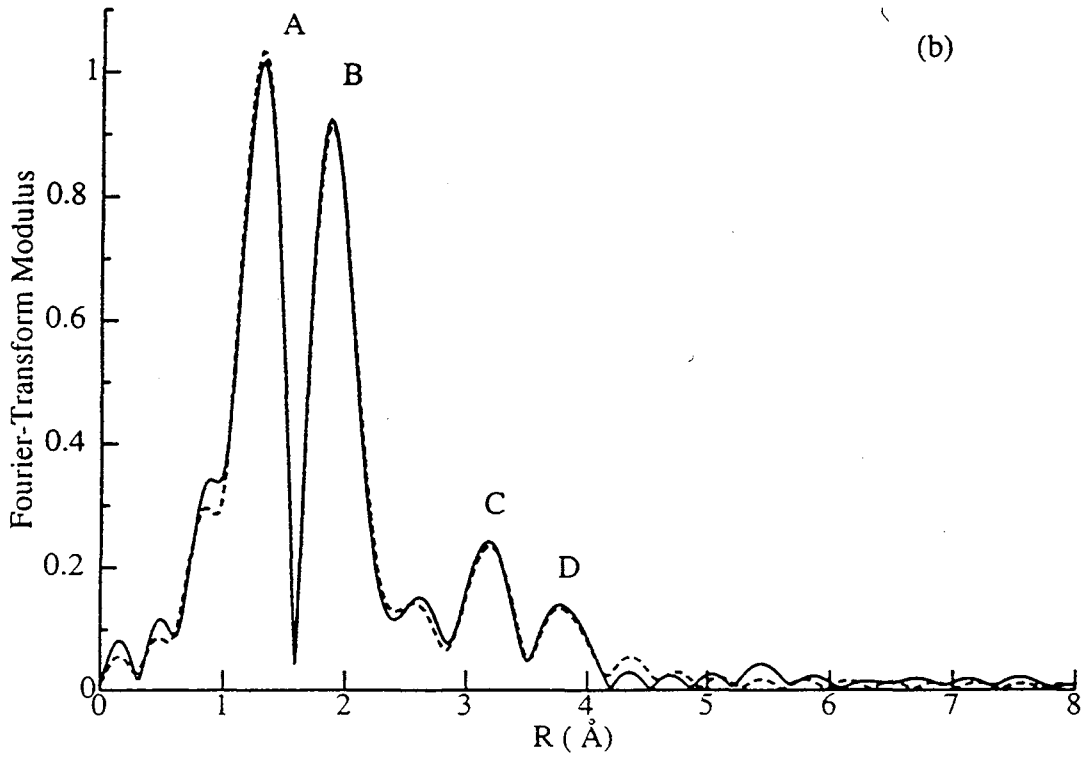

Figure 7

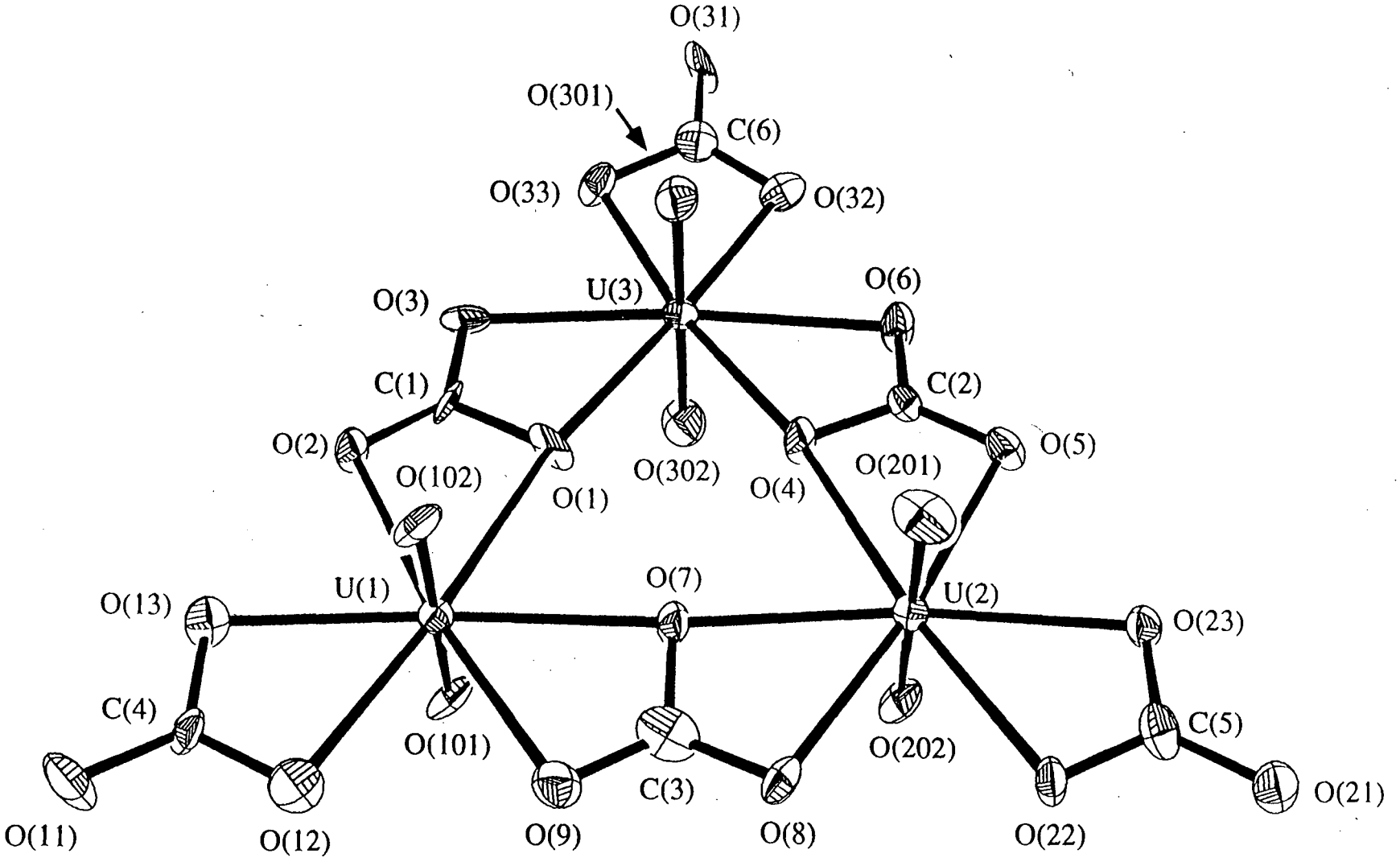
O(31)
O(301)
C(6)
O(33)
O(32)
O(3)
U(3)
O(6)
C(1)
C(2)
O(2)
O(102)
O(1)
O(302)
O(4)
O(201)
O(5)
U(1)
O(7)
U(2)
O(13)
O(23)
C(4)
O(101)
O(202)
C(5)
C(3)
O(21)
O(11)
O(12)
O(9)
O(8)
O(22)

Figure 8

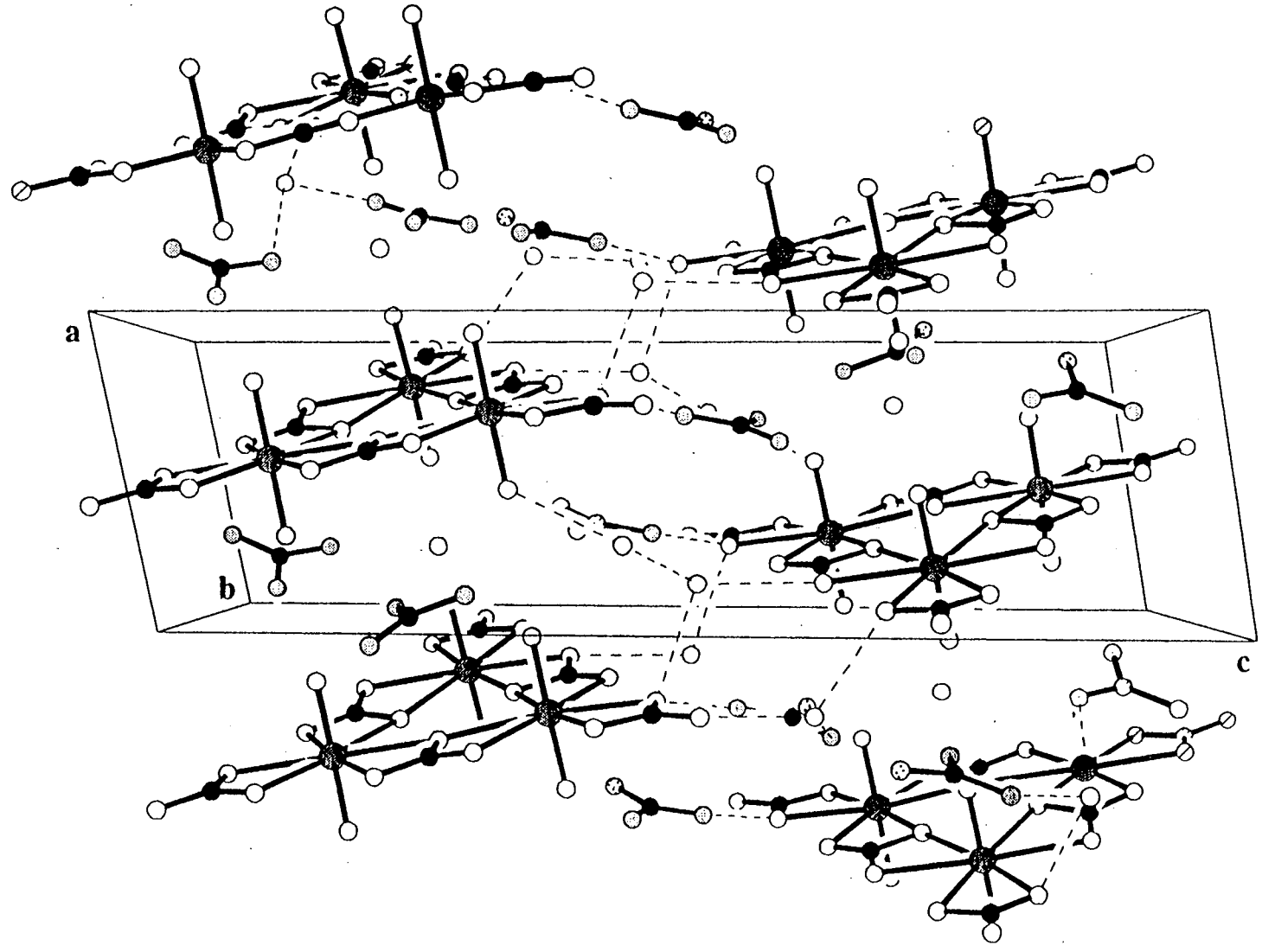

Figure 9

LAWRENCE BERKELEY LABORATORY
UNIVERSITY OF CALIFORNIA
TECHNICAL INFORMATION DEPARTMENT
BERKELEY, CALIFORNIA 94720